Strain-level antigen variation facilitates immune evasion in *Bacteroides thetaiotaomicron*

Robert W.P. Glowacki[1,2], Jessica M. Till[1,2,3], Orion D. Brock[1,2,3], Morgan J. Engelhart[1,2,3,4], Philip P. Ahern[1,2,3]

[1]Department of Cardiovascular and Metabolic Sciences, Lerner Research Institute, Cleveland Clinic, Cleveland, OH 44195, USA;

[2]Center for Microbiome and Human Health, Lerner Research Institute, Cleveland Clinic, Cleveland, OH 44195, USA;

[3]Department of Molecular Medicine, Cleveland Clinic Lerner College of Medicine, Case Western Reserve University, Cleveland, OH, USA;

[4]Currently, Department of Inflammation and Immunity, Lerner Research Institute, Cleveland Clinic, Cleveland, OH 44195, USA

Abstract

The T cell receptor (TCR) repertoire of intestinal CD4+ T cells is enriched for specificity towards microbiome-encoded epitopes shared among many microbiome members, providing broad microbial reactivity from a limited pool of cells. These cells actively coordinate mutualistic host-microbiome interactions, yet many epitopes are shared between gut symbionts and closely related pathobionts and pathogens. Given the disparate impacts of these agents on host health, intestinal CD4+ T cells must maintain strain-level discriminatory power to ensure protective immunity while preventing inappropriate responses against symbionts. However, to date, the mechanisms by which this occurs have remained enigmatic. To interrogate this, we leveraged BθOM mice that express a transgenic TCR specific for a *BT4295*-encoded epitope in *B. thetaiotaomicron*. While many *B. thetaiotaomicron* strains potently activated BθOM CD4+ T cells *in vitro*, strain dnLKV9 escaped recognition. Bioinformatic analyses uncovered two *BT4295* homologs in *B. thetaiotaomicron*-dnLKV9, with each homolog harboring sequence modifications relative to strain VPI-5482, specifically a premature stop codon and a T548S substitution within the epitope. Reconstruction of these variants in *B. thetaiotaomicron*-VPI-5482$^{\Delta BT4295}$ conferred evasion from BθOM CD4+ T cells *in vitro* to this otherwise permissive strain. Adoptive transfer of BθOM CD4+ T cells to gnotobiotic RAG1-/- colonized with *B. thetaiotaomicron* harboring these variant *BT4295* forms verified the sufficiency of these antigen modifications for evasion of BθOM CD4+ T cells. Collectively, these data uncover the existence of strain-level immune evasion in *B. thetaiotaomicron* and reveal a mechanism whereby strains evade recognition by CD4+ T cells, facilitating strain-level discrimination in responsiveness to the microbiome.

Running Title

Strain-level immune evasion in *B. thetaiotaomicron*

Key Points

-Select *B. theta* strains evade recognition by a *B. theta*-specific CD4+ T cell

-Strain-specific antigen modifications rather than absence of antigen mediate evasion

-Evasion strategies limit *in vivo* accumulation of *B. theta*-specific CD4+ T cells

Introduction

The intestine is home to a complex microbial ecosystem, the gut microbiome, that contributes to organismal health [1-3]. The network of intestinal immune cells is continuously exposed to microbial products to which they must remain tolerant. CD4+ T cells play an integral role in maintaining intestinal homeostasis through their capacity to adopt specialized functions that both regulate inflammatory responses and limit the penetration of microbial products into the lamina propria [1, 2, 4-8]. As such, a variety of microbiome members can coordinate the development of intestinal Th1, Th2, Th17 [9-12], regulatory (Treg) [13-18] or follicular helper (Tfh) T cells [19, 20] that ensure the maintenance of mutualistic interactions with the microbiome. Although these microbes can promote environments that are conducive to differentiation of CD4+ T cell subsets irrespective of whether the cells are specific for antigens from the inciting microbe [21-23], several studies have demonstrated that the CD4+ T cell populations induced by these microbiome members express T cell receptors (TCR) that are specific to antigens derived from these agents [19, 20, 24-37]. For example, Segmented Filamentous Bacteria (SFB) is a potent inducer of Th17 cells in the small intestinal lamina propria, and the Th17 cells triggered by SFB harbor TCRs that are specific for SFB antigens [9, 10, 24, 27]. Similarly, several species of *Helicobacter* can drive the development of Treg responses in the colonic lamina propria, and this is associated with the emergence of *Helicobacter*-specific T cells within the Treg pool [25, 26, 30]. Thus, specific cellular fates are tied to TCR specificity for members of the microbiome, thus linking the functions of a given T cell subset to the presence of individual microbes.

However, this presents challenges for intestinal CD4+ T cells. The large number of potential epitopes that can be derived from the gut microbiome is enormous and although there need not be a T cell clone specific for every epitope, the extraordinary epitope diversity coupled to constraints on the size of the CD4+ T cell compartment, dictate a need for an efficient system that balances the requirement for reactivity to a broad array of microbes with a limited number of cells. The concept of immunodominance of particular epitopes [38] and the inherent cross-reactivity of the TCR [39] represent mechanisms through which the constrained size of the intestinal T cell compartment could possess reactivity to multiple microbiome members (i.e. not all theoretical epitopes will be responded to, and one cell could recognize multiple epitopes). However, early studies showing that microbiome-derived immunodominant epitopes could be shared among phylogenetically related microbes [28, 29] provided an additional potential explanation for how a limited set of CD4+ T cells could retain activity to a broad microbial community through recognition of many microbes via a single TCR-epitope pair. Indeed, a systematic assessment of the specificities among intestinal T cells showed that the TCR pool in intestinal CD4+ T cells is dominated by TCRs that are specific for epitopes that are widely shared and broadly distributed across multiple members of the microbiome [40]. Collectively, these studies provide a conceptual framework to understand how the intestinal CD4+ T cell compartment can retain reactivity to a broad array of microbes despite the constraints on the number of T cell clones that can be maintained.

Despite the utility of this model, it does not adequately account for the need to tailor the quality of the CD4+ T cell response in a highly specific manner, often at the level of the individual strain from which the epitope is derived. For example, different strains of gut microbiome species will have substantial genomic similarity yet may impart distinct effects on the host, with some mediating beneficial functions while others have deleterious effects, exemplified by toxigenic

and non-toxigenic strains of *Bacteroides fragilis* [41-45]. Indeed, there is potentially significant antigen overlap between gut symbionts and overt pathogens as is evidenced by the existence of gut-resident commensal strains of *Escherichia coli* and related enteropathogenic *E. coli* and *Shigella* [46, 47]. Thus, intestinal CD4+ T cells must maintain the capacity to deploy their inflammatory function in response to some microbes and tolerogenic properties in response to others, even if two such agents share the same epitope. However, how such discriminatory power is achieved has remained unclear. Indeed, whether or not all strains that genomically encode an epitope elicit responsiveness of T cell clones specific for the epitope, and promote the same quality of response, is largely unknown.

One reason for these limitations has been a lack of systems to adequately interrogate these questions. Although people have used heterologous expression of defined T cell epitopes in different bacteria to determine the impact on intestinal T cell responses [27, 48], the dearth of information regarding naturally existing shared epitopes in genetically tractable gut microbes has limited progress in this area. Here we have leveraged the BθOM TCR transgenic mouse line which expresses an I-A^b-restricted TCR specific for a defined epitope present in the gut symbiont *Bacteroides thetaiotaomicron* (*B. theta* hereafter) [32]. The combination of transgenic TCR clone and the array of strains of *B. theta* with sequenced genomes, coupled with its genetic tractability facilitate the high-resolution required to define antigen variation across strains and how it impacts detection by CD4+ T cells. Using this system, we found that genomic encoding of the epitope recognized by BθOM CD4+ T cells by different *B. theta* isolates was not sufficient for T cell activation, and that strain *B. theta*-dnLKV9 lacked the capacity to stimulate BθOM CD4+ T cells at levels above that of a *B. theta* strain deficient in the epitope, despite expression of the gene at levels equivalent to strains that were potent stimulators of BθOM CD4+ T cells. Using a CD4+ T cell transfer system in gnotobiotic RAG1-/- mice, we found that this strain also failed to provide stimulation to these cells *in vivo* validating the evasion of BθOM CD4+ T cells by *B. theta*-dnLKV9. Bioinformatic interrogation of the genome of *B. theta*-dnLKV9 uncovered: (i) the presence of a premature stop codon downstream of the epitope recognized by BθOM CD4+ T cells, and (ii) the existence of an additional homolog of *BT4295*, present at a distinct locus in the genome that harbored a substitution, T548S, that severely impacted the capacity of the epitope to stimulate BθOM CD4+ T cells. Reconstruction of these two forms of the antigen in a strain background that supports stimulation of BθOM CD4+ T cells, but where endogenous *BT4295* had been deleted, confirmed that these sequence variations were sufficient to confer the BθOM CD4+ T cell evading properties of *B. theta*-dnLKV9. These data uncover the existence and mechanistic basis through which strains may evade CD4+ T cell responses specific for epitopes they encode. Thus, while these data suggest that individual T cell clones may recognize many gut bacterial strains, the constellation of clones that are specific for a strain will be unique, thus providing a means through which species-specific clones and strain-specific clones allow recognition of a broad array of microbes while retaining strain-level resolution in the ensuing responses as needed.

Materials and Methods

Mice: C57BL/6J (Jackson Labs, strain # 000664) were purchased from Jackson Labs as needed and allowed to acclimatize in a non-barrier facility for at least 1 week prior to use. BθOM mice were provided to us by Paul Allen (Washington University in St. Louis) and maintained in-house following rederivation in a non-barrier facility. BθOM mice were on a RAG1-/- CD45.1+/+CD45.2-/- background. Conventional mice (non-gnotobiotic) were housed in a non-barrier facility under a 14 hour light and 10 hour dark cycle, and provided with food (LabDiet, Cat. # 5010 - Laboratory Autoclavable Rodent Diet) and water *ad libitum*. Breeder mice were fed irradiated Teklad global 19% protein extruded diet (Teklad Laboratory Animal Diets, Cat. # 2019) and at weaning mice were switched to irradiated 2018 Teklad Global 18% Protein Rodent Diet (Teklad Laboratory Animal Diets, Cat. # 2018). Cages contained 1/8 inch corncob bedding and nestlets were provided for enrichment. The following agents are tolerated in this facility: Mouse Norovirus (MNV), Murine Chapparvoviruses (MuCPV/MKPV), *Helicobacter* spp., *Corynebacterium bovis*, *Rodentibacter* spp., *Entamoeba muris*, and *Tritrichomonas* spp. RAG1-/- (B6.129S7-Rag1tm1Mom/J; Jackson Labs, strain # 002216) were purchased from Jackson Labs and rederived as germ-free in-house, and a germ-free colony was maintained by intercrossing RAG1-/- mice. Germ-free mice were bred in plastic flexible film isolators (Class Biologically Clean, Ltd., Madison, WI) under a 14 hour light and 10 hour dark cycle. Food (LabDiet, Cat. # 5021 for breeder mice and Cat. # 5010 for weaned mice) and water were provided *ad libitum.* For germ-free mice, all food, bedding, and water (non-acidified) were sterilized by autoclaving. Cages contained ALPHA-dri Plus Bedding (Shepherd Specialty Papers, Cat. # ALPHA-dri+PLUS), and paper towels were provided for enrichment. Sterility of germ-free mice breeding in isolators is ascertained monthly by the Gnotobiotics Facility using tests that rotate between aerobic and anaerobic cultures on rich media, Gram stains of fecal smears, and 16S rRNA PCR. In addition, mold traps are also maintained in each isolator. Mice were housed in Allentown Sentry Sealed Positive Pressure cages (Allentown) which were held in an Allentown Housing Unit for execution of experiments. All experiments and procedures were approved by the Institutional Animal Care and Use Committee (IACUC) of the Cleveland Clinic Foundation. Both male and female mice were used for experiments shown.

Media formulations for murine cells: All assays involving the culture of murine cells were performed in “complete” Roswell Park Memorial Institute Medium (RPMI) that was formulated as follows: RPMI 1640 supplemented with HEPES, Fetal Bovine Serum, penicillin/streptomycin, and 2-mercaptoethanol as indicated in the table below. Media was sterilized by passing through a 0.22 micron filter (Fisher Scientific, Cat. # FB12566510) to sterilize prior to use. For the isolation of cells from the colon, “digestion RPMI” was prepared in the same manner as complete RPMI but 2-mercaptoethanol was not added and the media was not filter-sterilized.

Reagent Name	Supplier, Cat. #	Final Concentration in Media
RPMI 1640	Prepared in-house from Gibco, Cat. # 31800-105	N/A

Penicillin/Streptomycin	Prepared in-house from Penicillin-G, Sigma, Cat. # P3032-100 and Streptomycin, Gibco Cat. # 11860-038	50 Units/mL for each antibiotic
Fetal Bovine Serum (Heat Inactivated)	Gibco, Cat. # 10437028	5-10% v/v
HEPES	Gibco, Cat. # 15630-080	20 mM
2-Mercaptoethanol	Sigma, Cat. # M3148-100ML	50 μM

CD4+ T cell isolation: CD4+ T cells used for *in vitro* assays and *in vivo* transfer experiments were isolated from the spleen. Spleens were harvested and stored on ice in $Ca2^{+}$-free and $Mg2^{+}$-free phosphate buffered saline (PBS) (prepared in-house from Caisson, Cat. # PBP01) supplemented with 0.1% w/v bovine serum albumin (BSA) (Sigma, Cat. # A3059-500G) (PBS/BSA hereafter). Splenocytes were isolated as previously described [49]; briefly, spleens were physically forced through 70 micron (Falcon; Cat. # 352350) or 100 micron (Falcon; Cat. # 352360) sterile cell strainers, and pelleted by centrifugation at 453 X g for 5 minutes. The supernatant was decanted and red blood cells were lysed by addition of ~750 microlitres pre-warmed (37C) ammonium-chloride-potassium (ACK) lysis buffer (Gibco, Cat. # A10492-01) followed by immediate mixing. After 3 minutes lysis was halted by adding ~10 mL of PBS/BSA to each tube, and cells were filtered through a 70- or 100-micron sterile cell strainer and centrifuged at 453 X g for 5 minutes. Supernatant was poured off and pellet resuspended for downstream use. For *in vitro* BθOM CD4+ T cell isolation, naïve CD4+ T cells were enriched for using the Miltenyi Mouse Naïve CD4+ T cell Purification Kit (Miltenyi Biotec, Cat. # 130-104-453) as per the manufacturer's instructions. For *in vivo* transfer experiments, wild-type CD4+ T cells were isolated using the Miltenyi Mouse CD4+ T cell isolation kit (Miltenyi Biotec, Cat. # 130-104-454) as per the manufacturer's instructions. For *in vivo* transfer of BθOM CD4+ T cells, splenic naïve CD4+ T cells were purified as $CD4^{+}TCRV\beta12^{+}CD45.1^{+}CD25^{-}CD44^{lo}CD62L^{+}$ or $CD4^{+}TCRV\beta12^{+}CD45.1^{+}CD45.2^{-}CD25^{-}CD44^{lo}CD62L^{+}$ using a FACSAria Fusion cell sorter. All steps in preparation of wild-type and BθOM CD4+ T cells for transfer *in vivo* were performed in PBS/BSA supplemented with penicillin/streptomycin as per complete RPMI. Cells were purified using a FACSAria Fusion cell sorter, and sorted into complete RPMI (10% v/v fetal bovine serum). The purity of CD4+ cells ranged from ~91-94% (see **Fig S1** for examples of pre- and post- sorting). Of the purified CD4+ T cells, ~95%-97% were $CD25^{-}CD44^{lo}CD62L^{+}$. Wild-type CD4+ T cells and BθOM CD4+ T cells were both washed twice in PBS by pelleting at 453 X g for 5 minutes, decanting of supernatant and resuspending the pellet in ~15 mL of PBS. Cells were mixed at a ratio of ~95% wild-type CD4+ T cells wild-type plus ~5% BθOM CD4+ T cells in PBS. Cells were transferred via the retro-orbital route as follows: mice were anesthetized using isoflurane, a drop of proparacaine hydrochloride 0.5% (Bausch + Lomb, Cat. # NDC24208-730-06) was administered to the eye to be injected prior to injection, cells were then injected in a volume of 150 microlitres, following which an additional drop of proparacaine hydrochloride was administered.

Bone Marrow-Derived Dendritic Cell (BMDC) Preparation: To generate BMDC, the bone marrow of wild-type C57BL/6J mice was isolated, red blood cells were lysed following the same procedure used for spleens (with 7 minute centrifugation steps), using a volume of 1 mL ACK lysis buffer to lyse red blood cells. Bone marrow cells were then seeded in a polystyrene Petri dish (Fisher, Cat. # FB0875712) at a density of 2 X 10^{6} cells in 10 mL complete RPMI 1640

supplemented with 20 ng/mL granulocyte-macrophage colony-stimulating factor (GM-CSF) (PeproTech, Cat. # 315-03) on Day 0. On Day 3 an additional 10 mL of complete RPMI supplemented with 20 ng/mL GM-CSF was carefully added with gentle swirling to mix. On Day 6 and Day 9, 10 mL was withdrawn from the edge of each plate, centrifuged at 453 X g for 5 minutes, supernatant removed and the pellet resuspended in 10 mL of complete RPMI supplemented with 10 ng/mL or 5 ng/mL GM-CSF respectively, and 10 mL added back to the plate followed by gentle swirling of the Petri dish to mix. Cells were harvested for use in assays from Day 10-11 by pipetting of non-adhered/loosely adhered cells, centrifugation at 453 X g, discarding supernatant and resuspending the pellet in complete RPMI or PBS, pelleting again at 453 X g, removing supernatant and resuspending cells in complete RPMI for use in downstream assays.

<u>Bacterial growth and genetic manipulation of *B. theta* stains:</u> *B. thetaiotaomicron* strains were routinely grown in tryptone-yeast extract-glucose (TYG) media (see below for components) that was sterile filtered prior to use using a 0.22 micron filter unit (Fisher Scientific, Cat. # FB12566510) and allowed to equilibrate in an anaerobic chamber (Coy Laboratory, Grass Lake, MI; atmosphere 10% carbon dioxide, 5% hydrogen, balance nitrogen) for 2 days prior to use. For maintenance of *B. thetaiotaomicron* on solid media, brain-heart-infusion (BHI)-blood agar plates were prepared in Petri dishes (Fisher, Cat. # FB0875712) by autoclaving BHI Broth (BD, Cat. # 211059) and agar (Fluka, Cat. # BP1423) that had been mixed with MilliQ water up to 90% of the desired end volume, followed by the addition of defibrinated horse blood (Quad Five, Cat. # 210-500) to a final concentration of 10% v/v once media had cooled to ~60°C after autoclaving. Where necessary for genetic manipulation antibiotics and selective compounds were added to BHI-blood plates as follows: 200 µg/mL gentamicin (Gibco, Cat. # 15750060), 25 µg/mL erythromycin (Sigma, Cat. # E5389), and 200 µg/mL 5-fluoro-2'-deoxyuridine (FUdR) (Matrix Scientific, Cat. # 0089451G). *E. coli* strains used in genetic manipulation of *B. thetaiotaomicron* were grown overnight aerobically with agitation at 200 rpm in lysogeny broth (LB) broth Millers modification (Fisher Scientific, Cat. # BP1426) with 300 µg/mL of ampicillin (Sigma, Cat. # A9518) added. In-frame genetic manipulation of *B. thetaiotaomicron* strain VPI-5482 were done via allelic exchange through homologous recombination using pExchange as described previously [50]. Briefly, all manipulations in VPI-5482 were done in a strain lacking thymidine kinase (Δ*tdk*) as well as*BT4295* (Δ*BT4295*) [32] to facilitate counter-selection using the toxic drug, FUdR (102) and to insert different constructs of *BT4295* with the desired modifications to the epitope. Briefly, S17 *E. coli* λpir harboring the plasmid/construct of interest and *B. thetaiotaomicron* strains were grown separately overnight and then subcultured the following day and grown to an OD_{600} of ~0.6-0.8 representing a mid-log phase of growth. At this point the *E. coli* and *B. thetaiotaomicron* were combined, centrifuged at 8,000 x g for 5 minutes and resuspended in 1 mL of PBS. This resuspension was then plated on BHI-blood plates with no antibiotic added and incubated at 37°C aerobically to allow for the conjugative transfer of the plasmid from *E. coli* into *B. thetaiotaomicron*. After ~16 hr of incubation, the resulting dense lawn of bacteria was scraped from the plate and resuspended in PBS before being plated on BHI-blood plates containing gentamicin to select for only *B. thetaiotaomicron* species (the *E. coli* strain used is susceptible to gentamicin) and erythromycin to select for positive *B. thetaiotaomicron* transformants harboring the appropriate plasmid, plates were incubated anaerobically for three days. Following this, individual colonies were picked into TYG without antibiotics and grown overnight in liquid media (these represent the merodiploid stage) these

251 were then plated on BHI-blood plates containing 200 ug/mL FUdR as a counter-selection as
252 those cells that have not lost the plasmid (which encodes a copy of the thymidine kinase gene)
253 will be unable to grow at this stage due to FUdR toxicity in the presence of a functional
254 thymidine kinase gene. Individual colonies were then grown in TYG and DNA isolated and
255 screened by PCR and Sanger sequencing to confirm gene deletions. All strains, primers, and
256 plasmids are listed in **Table S1**.

257

258 **TYG Media**

Reagent Name	Supplier, Cat. #	Final Concentration in Media	Notes
Tryptone Peptone	Gibco, Cat. # 211921	10 g/L	
Bacto Yeast Extract	BD, Cat. # 212750	5 g/L	
Glucose	Sigma, Cat. # G8270	2 g/L	
Cysteine HCl	Sigma, Cat. # C1276	0.5 g/L	Added last and media placed in the anaerobic chamber promptly after addition
1M Potassium Phosphate Buffer (pH 7.2)	Prepared in-house from 1M potassium phosphate monobasic (Sigma, Cat. # P0662), and 1M potassium phosphate dibasic (Sigma, Cat. # P3786)	100 mL/L	Potassium phosphate monobasic potassium phosphate dibasic were prepared in water
Vitamin K_3 (menadione) (1 mg/mL stock)	Sigma, Cat. # M5625	1 mL/L of 1 mg/mL stock	Stock prepared in 100% ethanol
TYG Salts	Prepared in-house as per table below	40 mL/L	
$FeSO_4$ (0.4 mg/mL stock)	Sigma, Cat. # F8048	1 mL/L of a 0.4 mg/mL stock	Stock prepared in water
$CaCl_2$ (8 mg/mL stock)	Sigma, Cat. # C7902	1 mL/L of an 8 mg/mL stock	Stock prepared in water
Hemin (10 mg/mL stock)	Sigma, Cat. # 51280	0.5 mL/L of a 10 mg/mL stock	Stock prepared in 0.1 N NaOH
Vitamin B_{12} (0.01 mg/mL stock)	Sigma, Cat. #V2876	0.5mL/L of a 0.01 mg/mL stock	Stock prepared in water

259

260

261

262 **TYG Salts**

Reagent Name	Supplier, Cat. #	Final Concentration in Media	Notes
$MgSO_4 \cdot 7H_2O$	Sigma, Cat. # M63-500	0.5 g/L stock	Stock prepared in water
$NaHCO_3$	Sigma, Cat. # S4019	10 g/L stock	Stock prepared in water
NaCl	Sigma, Cat. # S3014	2 g/L stock	Stock prepared in water

263

264 Preparation of bacteria for *in vitro* assays

265 To prepare bacteria for *in vitro* assays, *B. thetaiotaomicron* strains were grown overnight in TYG
266 media to stationary phase as described above. 1 mL was pelleted by centrifugation at 10,000 x
267 g, supernatant removed, pellet resuspended in PBS, cells pelleted again by centrifugation at
268 10,000 x g and supernatant removed. Cells were then resuspended in 1 mL PBS and heat-killed
269 by incubation at 95°C for 90 minutes. Prior to use in assays, cells were pelleted and
270 resuspended in the appropriate volume of complete RPMI and normalized using OD_{600}. For
271 graphs showing *in vitro* activation with OD_{600} equivalent units on the x-axis, these values
272 represent the total OD_{600} equivalent units present in the well at the indicated value, i.e. if a
273 culture of *B. theta* had an OD_{600}=4, then 50 microlitres of culture, washed and added to a well
274 with a final end volume of 200 microlitres following addition of BθOM CD4+ T cells would
275 represent and OD_{600} unit of 1 in a well.

276

277 Colony forming unit (CFUs) assay

278 Enumeration of CFUs from bacterial cultures was performed by spot-dilution plating on BHI-blood
279 agar plates prepared as above with addition of 200 µg/mL gentamicin (Gibco, Cat. # 15750060).
280 10 µL of overnight culture was normalized to an OD_{600} of 1.0 and serially diluted 1:10 and then 10
281 µL of these dilutions were spot plated onto plates in technical duplicate and allowed to incubate
282 48-72 hours anaerobically followed by visual counting of colonies. Colony forming unit (CFU)
283 enumeration from *in vivo* transfer experiments was performed as follows: flash frozen fecal pellets
284 were weighed in a tared 2 mL microcentrifuge tube and resuspended at 100 mg/mL in PBS
285 followed by agitation via pipetting, vortexing, and manual disruption of the pellet using a sterile
286 wood applicator. Particulate matter was allowed to settle ~5-10 minutes at room temperature.
287 1:10 serial dilutions were performed and spot plated on BHI-blood plates and incubated for 48-96
288 hours.

289

290 Quantitative Reverse Transcriptase PCR measurements of *BT4295*

291 *B. thetaiotaomicron* strains were grown overnight in sterile pre-reduced TYG, subcultured 1:100
292 into 5 mL of fresh TYG media the next day and grown to stationary phase (OD_{600} of ~1.2-1.6) in
293 TYG. 1.5 mL of cells were then spun down at 8,000 x g for 3 minutes, resuspended in 500 µL
294 ribonucleic acid (RNA) protect bacterial reagent (Qiagen, Cat. # 76506), allowed to incubate at

295 room temperature for 10 minutes followed by centrifugation at 5,000 x g for 10 minutes. RNA
296 protect was removed and the pellets were stored at −80°C until processed further. Total RNA
297 was extracted using buffers from the RNeasy Mini Kit (Qiagen) and purified on RNA-binding
298 spin columns (Epoch Life Science, Cat. # 1940-250). Purified RNA was treated with 4 units of
299 DNase I (1µL/unit) (NEB, Cat. # M0303) for 1 hour at 37°C. After DNase inactivation using 4 µL
300 of 0.5 M ethylenediaminetetraacetic acid (EDTA) (Thermo Fisher Scientific, Cat. #AM9260G),
301 RNA was purified again using a second RNA-binding spin column. Reverse transcription was
302 performed using SuperScript III reverse transcriptase (Invitrogen, Cat. # 18080093) and random
303 primers (Invitrogen, Cat. # 48190011). The abundance of each target *BT4295* homolog
304 transcript in the resulting cDNA was quantified by quantitative PCR using an in-house qPCR mix
305 as previously described [51]. Briefly, each 20 µL reaction contained 1X Thermopol Reaction
306 Buffer (NEB, Cat. # B9004S), 125 µM dNTPs (Thermo Fisher Scientific, Cat. # 10297018), 2.5
307 mM MgSO4 (NEB, Cat. # B1003S), 1X SYBR Green I (Lonza, Cat. # 50513), 500 nM gene
308 specific or 65 nM 16S rRNA primer specific to *Bacteroides* species [50] and 0.5 units Hot Start
309 Taq Polymerase (NEB, Cat. # M0495S). 10 ng of template cDNA was used per reaction. To
310 determine gene expression levels, the expression of the 16S rRNA was used as a
311 housekeeping gene, and fold change was calculated relative to those obtained for the type
312 strain, VPI-5482 using the ΔΔCT method. Primers are listed in **Table S1**.

313 *In vitro* BθOM CD4+ T cell assays: To determine the capacity of various strains of *B. theta* to
314 stimulate BθOM CD4+ T cells, BMDC were prepared as above and incubated with heat-killed *B.*
315 *theta* at a variety of doses overnight at 37°C in a volume of 100 microlitres of complete RPMI in
316 a humidified incubator supplemented with 5% C02. Incubations were performed in flat-bottomed
317 96 well plates (Falcon, Cat. # 353072). BθOM CD4+ T cells were isolated as described above
318 and added in a volume of 100 microlitres with BMDC (1:1 ratio of T cells and BMDC) and mixed
319 by pipetting. 2 days later cells were prepared for flow cytometric-based analysis. The precise
320 number of cells seeded varied depending on yield, from ~$5X10^4$-$1X10^5$ of each cell type per
321 well. Cell numbers were identical for all groups in a given experiment. For experiments showing
322 stimulation with synthetic peptides, the wild-type (EEFNLPTTNGGHAT) and T548S
323 (EEFNLPTSNGGHAT) forms of the peptides were commercially synthesized (GenScript) and
324 purified (>98% purity) and added to wells at the indicated concentrations overnight as for
325 bacteria prior to the addition of BθOM CD4+ T cells. Independent experiments were represented
326 by distinct sets of BMDC, BθOM CD4+ T cells and batches of heat-killed bacteria.

327

328 Isolation of colonic cells

329 To isolate cells from the colon for phenotyping, colons were extracted immediately after
330 euthanasia, opened longitudinally, and rinsed in PBS/BSA by vigorous swirling. Colons were
331 then chopped into 4-5 pieces and stored in ~10 mL of PBS/BSA in a 50 mL tube (Falcon, Cat. #
332 352070) on ice until ready for further processing. To remove epithelial cells and intraepithelial
333 lymphocytes, the majority of the PBS/BSA solution was removed (residual buffer remained to
334 ensure the tissue was fully immersed in liquid) and ~15 mL of PBS supplemented with EDTA
335 (final concentration 5 mM; Corning, Cat. # 10823013) was added (PBS/EDTA hereafter). Tubes
336 were placed laterally in an orbital shaker and incubated at 37°C with rotation of 180 rpm for 15-
337 20 minutes. Tubes were then vigorously shaken for ~30 seconds, tissue was allowed to settle
338 and the majority of the PBS/EDTA was removed. An additional 15-20 mL of PBS/EDTA was

339 added and the incubation step repeated. Tubes were again vigorously shaken for ~30 seconds,
340 following which the tissue was removed, briefly dunked in PBS/BSA before being minced with
341 razor blades. To remove residual EDTA the minced tissue was then placed in a 50 mL tube
342 containing ~10 mL of digestion RPMI (complete RPMI without addition of 2-mercaptoethanol),
343 and the tube was gently inverted to mix. After 5 minutes of incubation, the majority of the
344 digestion RPMI was removed and a fresh ~10 mL of digestion RPMI added, tube was gently
345 inverted to mix and then allowed to sit at room temperature for 5 additional minutes. The
346 majority of the digestion RPMI was removed and 10 mL of digestion RPMI supplemented with
347 0.1 mg/mL Collagenase Type VIII (Sigma, Cat. # C2139) and 0.075 U/mL Dispase (Corning,
348 Cat. # 345235) was added. Tubes were placed laterally in an orbital shaker and incubated at
349 37°C with rotation of 180 rpm for 30 minutes. Following this incubation, tubes were vortexed for
350 ~30 seconds, tissue allowed to settle and the majority of the digestion RPMI was harvested, and
351 passed through a 70 micron cell strainer into a fresh 50 mL tube. The remaining tissue
352 underwent a second identical round of digestion with digestion RPMI supplemented with
353 collagenase type VIII and dispase. The harvested digestion media was pooled with that of the
354 first digestion by passing through a 70 micron cell strainer, and ~15 mL PBS/EDTA was added
355 to halt the digestion. Cells were pelleted by centrifugation at 453 X g for 10 minutes, followed by
356 resuspension in ~45 mL PBS/BSA. Cells were again pelleted by centrifugation, supernatant
357 removed, and cells resuspended in the residual PBS/BSA volume in the tube, and stored on ice
358 until further use.

359

360 Flow cytometry

361 For flow cytometric based analysis, cells were placed in round bottom plates (Falcon, Cat. #
362 353077) and washed by centrifugation at 453 X g for 5 minutes, supernatant removed by flicking
363 the solution out of the plate. Cells were then resuspended by pipetting in 50 microlitres of a
364 solution of PBS/BSA containing anti-CD16/CD32 antibodies (clones 93 and 9E9; see table
365 below) and a fixable viability dye (see table below), and stored at 4C for 20-30 minutes. Cells
366 were then pelleted as described for the wash step, and resuspended by pipetting in 50
367 microlitres of a staining cocktail containing the relevant fluorophore-conjugated antibodies (see
368 table below), and stored at 4C for 20-30 minutes. Cells were then washed by addition of 200
369 microlitres PBS/BSA on top of the cells, followed by centrifugation and supernatant removal as
370 described above. This step was repeated two additional times, and cells were resuspended by
371 pipetting in 100 microlitres of a commercially available formaldehyde-based fixative (BioLegend,
372 Cat. # 420801) to fix the cells. Cells were stored overnight at 4C, and fixative was removed by
373 the addition of 200 microlitres PBS/BSA on top of the cells, followed by centrifugation at 652 x g
374 and supernatant removal as described above (note, centrifuge speed was increased once cells
375 were fixed). This step was repeated one additional time, and cells were resuspended in 200
376 microlitres PBS/BSA and acquired on an LSR Fortessa (BD Biosciences). Data were analyzed
377 in FlowJo software (Tree Star, version 10.10.0).

378 For cell isolation by flow cytometry, staining was performed similarly to described above, with
379 the following changes: (i) staining was performed in 50 mL tubes with cells resuspended at
380 ~$1X10^8$ cells/mL, (ii) Fc blocking reagents were not removed prior to incubation with
381 fluorophore-conjugated antibodies. Cells were purified by cell sorting on a FACSAria Fusion.

382

Antibody Target	Isotype	Clone	Fluorophore	Supplier; Cat. #	Concentration for staining
Anti-Mouse CD16/CD32	Rat IgG2a	93	None	BioLegend; 101302	5.0 µg/mL for cell sorting and phenotyping
Anti-Mouse CD16.2	Armenian Hamster IgG	9E9	None	BioLegend; 149502	5.0 µg/mL for cell sorting and phenotyping
Fixable Viability dye	N/A	N/A	Aqua	BioLegend; 423102	1/300 dilution following reconstitution as per manufacturer's instructions
Anti-Mouse CD45.2	Mouse (SJL) IgG2a	104	Alexa Fluor 700	BioLegend; 109822	1.67 µg/mL for phenotyping
Anti-Mouse CD45.2	Mouse (SJL) IgG2a	104	eFluor 450	ThermoFisher Scientific; 48-0454-82	1.0 µg/mL for cell sorting
Anti-Mouse CD45.1	Mouse (A.SW) IgG2a	A20	Alexa Fluor 488	BioLegend; 110718	2.5 µg/mL for cell sorting and 1.0 µg/mL for phenotyping
Anti-Mouse CD45.1	Mouse (A.SW) IgG2a	A20	PerCp-Cy5.5	BioLegend; 110728	0.67 µg/mL for phenotyping
Anti-Mouse CD4	Rat IgG2a	RM4-5	eFluor 450	ThermoFisher; 48-0042-82	0.67 µg/mL for phenotyping
Anti-Mouse CD4	Rat IgG2a	RM4-5	Brilliant Violet 605	BioLegend; 100548	1.0 µg/mL for cell sorting, 0.67 µg/mL for phenotyping
Anti-Mouse CD8a	Rat IgG2a	53-6.7	Brilliant Violet 510	BioLegend; 100752	1.0 µg/mL for cell sorting,
Anti-Mouse TCR-β	Armenian Hamster IgG	H57-597	Alexa Fluor 488	BioLegend; 109215	2.5 µg/mL for phenotyping
Anti-Mouse TCR-β	Armenian Hamster IgG	H57-597	APC	BioLegend; 109212	0.67 µg/mL for phenotyping
Anti-Mouse TCR-Vβ12	Mouse IgG1	MR11-1	Phycoerythrin (PE)	BioLegend; 139704	1.0 µg/mL for cell sorting, 0.67 µg/mL for phenotyping
Anti-Mouse CD25	Rat IgG1	PC61	Allophycocyanin (APC)	BioLegend; 102012	1.0 µg/mL for cell sorting

Anti-Mouse/Human CD44	Rat IgG2b	IM7	Alexa Fluor 700	BioLegend; 103026	2.5 µg/mL for cell sorting
Anti-Mouse CD62L	Rat IgG2a	MEL-14	PE-Cy7	BioLegend; 104418	1.0 µg/mL for cell sorting
Anti-Mouse CD69	Armenian Hamster IgG	H1.2F3	APC	BioLegend; 104513	0.67 µg/mL for phenotyping
Propidium Iodide	N/A	N/A	N/A	BioLegend; 421301	2.5 µg/mL for cell sorting

Comparative genomics of BT4295 homologs

Homolog alignment for BT4295 protein was performed by using NCBI protein-protein BLAST (Basic Local Alignment Search Tool) [52] (for the full amino acid sequence of BT4295 found in strain VPI-5482). The top BLAST results of 95% or greater similarity and at least 90% coverage were included in manual curation of a list of homologs, we confined our search to isolates and excluded sequences found in metagenomic datasets. With recent large depositions of *B. theta* isolates, our search still yielded over 100 hits with significant homology. We therefore limited our alignment to a subset of 36 isolates that were either present in our BLAST search or verified through Sanger sequencing to contain BT4295 with the BθOM T-cell epitope. Sanger sequencing was done on strains for which we have isolates of, and to distinguish between BT4295 homologs found in strain dnLKV9. Full protein sequences were downloaded and aligned in MegAlign Pro v.17.1.1 (DNASTAR, Inc) using the MUSCLE algorithm [53].

Statistical Analysis

Statistical analyses were performed using GraphPad Prism (version 10.2.1.). The specific statistical tests used are indicated within the figure legends. P values <0.05 were considered to be statistically significant.

411 **Results**

412 ***B. theta* strain dnLKV9 is not recognized by BθOM CD4+ T cells**

413 To investigate whether a given TCR that recognizes a microbiome-derived antigen would
414 provide the capacity to recognize all microbes that express the antigen, or whether particular
415 microbes may evade such recognition we leveraged the previously established "BθOM" TCR
416 transgenic mouse system [32]. BθOM mice express a transgene-encoded I-Ab restricted T cell
417 receptor (TCR) comprised of TCRVα1 and TCRVβ12 chains that recognizes an epitope
418 (EEFNLPTTNGGHAT) encoded by *BT4295* in the type strain, *B. theta*-VPI-5482. This TCR is
419 largely specific for *B. theta* as the epitope is not broadly distributed among members of the
420 *Bacteroides* [32], and its target is packaged into outer membrane vesicles (OMV) that mediate
421 its delivery across the gut epithelium [31]. Using an *in vitro* system, we set out to interrogate
422 whether the presence of *BT4295* (or homologs thereof) would confer the capacity to be detected
423 by BθOM CD4+ T cells. We therefore leveraged a panel of *B. theta* strains that carry a copy of
424 *BT4295* to probe this in an *in vitro* system. Bone-marrow derived dendritic cells (BMDC) were
425 pre-loaded with heat-killed strains of *B. theta* and mixed with naïve CD4+ T cells from BθOM
426 mice. The capacity of BθOM CD4+ T cells to recognize these isolates was then assessed by
427 measurement of CD69 expression on T cells, an early marker of T cell activation [54, 55], after 2
428 days of co-culture (**Fig 1A)**. Stimulation with the type strain of *B. theta* (VPI-5482) led to a dose-
429 dependent increase in the proportion of cells expressing CD69 as previously reported [32] (**Fig**
430 **1B and Fig S2)**. Stimulation with additional strains of *B. theta*, strain 0940-1 or 5951, induced
431 similar dose-dependent increases in CD69 expression, equivalent to the type strain, in keeping
432 with the idea that BθOM CD4+ T cells would be broadly reactive to isolates of *B. theta* (**Fig 1B**).
433 However, stimulation with strain dnLKV9 (described in [31, 56]) failed to elicit CD69 expression
434 to an appreciable degree. The expression of *BT4295* has been shown to be exquisitely sensitive
435 to components of the media in which *B. theta* is grown [32]. To exclude the possibility that *B.*
436 *theta*-dnLKV9 possessed the capacity to stimulate BθOM CD4+ T cells but simply had
437 differential nutritional cues/requirements for induction of *BT4295* expression compared to the
438 other strains tested, we measured the expression of *BT4925* by reverse transcriptase-
439 quantitative PCR (RT-qPCR) in stationary phase (this time-point was chosen for measurement
440 as this was the stage of the growth phase from which cells were harvested for use in stimulation
441 assays). Although *B. theta*-dnLKV9 expressed lower *BT4295* transcript than *B. theta*-strain 5951
442 (a potent activator of BθOM CD4+ T cells), its expression was equivalent if not greater than that
443 of *B. theta*-VPI-5482 (**Fig 1C**), thus excluding the possibility that a simple failure to transcribe
444 the gene could be responsible for the failure to stimulate BθOM CD4+ T cells.

445 To further test whether *B. theta*-dnLKV9 truly lacked the capacity to stimulate BθOM CD4+ T
446 cells, we utilized an *in vivo* model system whereby germ-free RAG1-/- mice were
447 monocolonized with *B. theta*-VPI-5482 or *B. theta*-dnLKV9. After ~2 weeks, all mice were
448 adoptively co-transferred with a mixture of unfractionated wild-type CD4+ T cells from a CD45.1-
449 CD45.2+ donor and naïve BθOM CD4+ T cells from a RAG1-/-CD45.1+CD45.2- donor (~95%
450 wild-type: ~5% BθOM) (**Fig 2A)**. The co-transfer of wild-type cells: (i) allowed us to compare the
451 fitness of BθOM CD4+ T cells relative to a reference population that should be unaffected by
452 capacity of the different strains to stimulate BθOM cells, thus providing an internal control for
453 each mouse, (ii) provided a control that allowed us to distinguish between issues affecting
454 reconstitution of transferred cells from direct results of antigen availability (the wild-type cells

455 should reconstitute mice regardless of the colonized microbes while the BθOM CD4+ T cells
456 depend on the presence of *BT4295*), and (iii) limited the potential that BθOM CD4+ T cells could
457 induce inflammatory responses against *B. theta* by providing a pool of regulatory T cells that
458 would limit such responses. ~3 weeks after cell transfer, BθOM (TCRVβ12+CD45.2- CD4+ T
459 cells) and wild-type CD4+ T cells (CD45.2+ CD4+ T cells) were quantified in the spleen and
460 colon of recipient mice. Strikingly, while wild-type cells readily accumulated in all mice in both
461 spleen and colon, *B. theta*-VPI-5482 colonized mice had significantly greater accumulation of
462 BθOM cells compared to *B. theta*-dnLKV9 (**Fig 2B-2E and Fig S2**). This was true both with
463 respect to the proportion of BθOM cells within the CD4+ T cell pool (**Fig 2B-2D**) as well as the
464 total number of BθOM CD4+ T cells (**Fig 2E)**, yet there were equivalent levels of colonization by
465 the two strains (**Fig 2F**). Despite the impaired accumulation of BθOM CD4+ T cells, the total
466 number of colonic CD4+ T cells (encompassing both wild-type and BθOM CD4+ T cells) did not
467 differ between the mice colonized with the two strains (**Fig 2G**), suggesting that the effects
468 observed with BθOM CD4+ T cells were not simply attributable to general differences in
469 reconstitution dynamics based on the strains. Thus, these data reinforce the results obtained
470 using our *in vitro* system and reveal that *B. theta*-dnLKV9 is significantly impaired in its capacity
471 to stimulate BθOM CD4+ T cells relative to other strains of *B. theta*.

472

473 ***B. theta* strain dnLKV9 harbors a variant copy of *BT4295***

474 We reasoned that the strain-level variation observed could reflect a strain-specific feature that
475 modulates immunogenicity, or that there may be alterations to the antigen itself or the epitope
476 within it. To explore this further, we examined the sequence of the *BT4295* homolog encoded by
477 *B. theta*-dnLKV9 (locus tag, C799_02394). As with *B. theta*-VPI-5482, the canonical epitope
478 recognized by the BθOM TCR (EEFNLPTTNGGHAT) was found in *B. theta*-dnLKV9 (**Fig 3**),
479 excluding the possibility that a lack of the epitope could explain the failure to be recognized by
480 BθOM CD4+ T cells. However, we noted a mutation downstream of the epitope that introduced
481 a premature stop codon, and this mutation was not evident in any of the other strains analyzed
482 (**Fig 3**). Were the protein to be translated and processed as normal, the epitope would be
483 expressed and would be expected to stimulate BθOM CD4+ T cells. Thus, we rationalized that
484 this premature stop codon impaired the proper maturation of the protein or its processing for
485 presentation of the epitope on MHCII. We first sought to revert this mutation within *B. theta*-
486 dnLKV9 such that the premature stop codon was removed, but our efforts to genetically modify
487 *B. theta*-dnLKV9 proved unsuccessful. To overcome these challenges, we utilized a system
488 whereby wild-type versions or variants of *BT4295* could be reconstituted in a *B. theta*$^{\Delta tdk \Delta BT4295}$
489 background (on the VPI-5482 background; the Δ*tdk* background facilitates counterselection
490 during construction of mutants of interest). Using the *in vitro* assay system described above, we
491 found that *B. theta*$^{\Delta tdk \Delta BT4295}$ reconstituted with wild-type *BT4295* (*B. theta*$^{\Delta tdk \Delta BT4295::BT4295}$) drove
492 CD69 expression in a dose-dependent manner in BθOM CD4+ T cells in our *in vitro* system
493 relative to *B. theta*$^{\Delta tdk \Delta BT4295}$ (**Fig 4A**), thus validating the approach. To determine if the
494 premature stop codon found in *B. theta*-dnLKV9 could explain the failure to stimulate BθOM
495 CD4+ T cells, we reconstituted *B. theta*$^{\Delta tdk \Delta BT4295}$ with a truncated form of *BT4295* that mimicked
496 the protein that would be formed due to the early stop codon in *B. theta*-dnLKV9 (*B.*
497 *theta*$^{\Delta tdk \Delta BT4295::\text{dnLKV9_trunc}}$) (note, although other amino acid differences exist between *BT4295* in
498 *B. theta*-VPI-5482 and its homolog in *B. theta*-dnLKV9, this construct represented the *B. theta*-

499 VPI-5482 form modified only to introduce the premature stop codon found in *B. theta*-dnLKV9;
500 amino acids downstream of the stop codon were deleted). Strikingly, as with *B. theta*-dnLKV9,
501 *B. theta*$^{\Delta tdk \Delta BT4295}$::dnLKV9_trunc failed to stimulate BθOM CD4+ T cell activation (**Fig 4B**). Thus,
502 although additional mechanisms may contribute to immune evasion in *B. theta*-dnLKV9, these
503 data demonstrate that the introduction of a premature stop codon as found in *B. theta*-dnLKV9,
504 in replacement of endogenous *BT4295* in *B.theta*-VPI-5482 is sufficient to confer the inability to
505 activate BθOM CD4+ T cells. Moreover, these data reveal that both *B. theta*-dnLKV9 and *B.*
506 *theta*$^{\Delta tdk \Delta BT4295}$::dnLKV9 were as defective as *B. theta*$^{\Delta tdk \Delta BT4295}$.

507

508 ***B. theta*-dnLKV9 harbors an altered version of the epitope recognized by BθOM CD4+ T**
509 **cells that facilitates immune evasion**

510 During our efforts to identify the *BT4295* homolog in *B. theta*-dnLKV9 we noted the existence of
511 a second gene (locus tag, C799_02504) coding for a product with significant homology to
512 *BT4295* that was present in a distinct locus (**Fig 3**; depicted in the figure as "dnLKV9 (T548S)").
513 Interestingly, this homolog is not present in *B. theta*-VPI-5482. Notably, this additional copy did
514 not possess the premature stop codon that could explain why it too did not contribute to the
515 activation of BθOM CD4+ T cells. However, it contained an altered version of the canonical
516 epitope with a T548S substitution when compared to the epitope found in *B. theta*-VPI-5482.

517 To determine if this additional copy represented an altered peptide ligand [57] for BθOM CD4+ T
518 cells we first tested the capacity of synthetic peptides representing the wild-type form of the
519 epitope (EEFNLPTTNGGHAT) or the T548S substituted form (EEFNLPTSNGGHAT; substitution
520 position underlined) to stimulate upregulation of CD69 *in vitro*. Strikingly, the T548S peptide was
521 severely impaired in its capacity to drive CD69 upregulation on BθOM CD4+ T cells using the *in*
522 *vitro* assay system described above. However, at the highest doses tested it was able to
523 promote a maximal CD69 expression at or nearly equivalent to maximum induced by the wild-
524 type form of the epitope (**Fig 5A**) (note, at the highest doses of WT peptide significant down-
525 regulation of the TCR was observed and thus some cells were not captured in our gating
526 strategy; inclusion of TCRβ- events showed almost identical results, not shown). Interestingly,
527 the T548S form did not interfere with the capacity of the wild-type form of the epitope to drive
528 upregulation of CD69 when BMDC were loaded with equivalent concentrations of both wild-type
529 and T548S forms of the peptide (**Fig 5A**). Thus, these data identify the existence of an altered
530 peptide ligand (APL) of the canonical epitope, and although of lower potency, the T548S
531 substituted form of the epitope did not possess BθOM inhibitory capacity, suggesting that it
532 lacks the antagonist function reported for many APL [58].

533 Next, we again leveraged our capacity to introduce modified forms of *BT4295* to *BT4295*-
534 deficient *B. theta*-VPI-5482 and generated a form that expressed *BT4295* with a T548S
535 substitution, *B. theta*$^{\Delta tdk \Delta BT4295}$::T548S. In addition, to determine if position 548 was a critical residue
536 for interaction of the BθOM TCR with *BT4295*, we generated additional mutants at this position,
537 specifically, T548A and T548V, and assessed their impact on activation of BθOM CD4+ T cells
538 in our *in vitro* assay system. Similarly to the synthetic peptide, we found that *B.*
539 *theta*$^{\Delta tdk \Delta BT4295}$::T548S displayed a severely impaired capacity to stimulate BθOM CD4+ T cells
540 relative to a *B. theta*$^{\Delta tdk \Delta BT4295}$::*BT4295* control, but could stimulate CD69 upregulation at higher
541 doses than required for *B. theta*$^{\Delta tdk \Delta BT4295}$::*BT4295* (**Fig 5B**) in keeping with the idea that this

542 mutation alters its potency as an agonist rather than ablating recognition completely. The T548A
543 substitution also severely impaired activation of BθOM CD4+ T cells, but the T548V mutation
544 had little effect or even enhanced activation (**Fig 5B**). Although the T548S mutant expressed a
545 lower amount of transcript than the control (**Fig 5C**), notably the expression was equivalent to
546 *BT4295* expression in strain 0940-1 which potently activated BθOM CD4+ T cells (**Fig 1C**).
547 Given this, the fact that the synthetic peptide produced similar results, and the magnitude of
548 reduction in activating capacity, this expression difference is not likely the reason for impaired
549 potency. Thus, our data shows that position 548 appears to be a critical residue in BT4295 for
550 recognition by BθOM CD4+ T cells, and modulation at this position has varying impacts on
551 stimulation of BθOM CD4+ T cells depending on the nature of the modification.

552 Modulation of the agonist potency has been linked to alterations to both the magnitude and
553 quality of the T cell response that ensues following T cell stimulation [59-67]. Given that the
554 T548S mutation impaired but did not abolish the capacity to stimulate BθOM CD4+ T cells we
555 wanted to determine if the mutation impacted the accumulation of BθOM CD4+ T cells and/or
556 their phenotype *in vivo*. We therefore used an experimental setup as described above, where
557 germ-free RAG1-/- mice were monocolonized with *B. theta*$^{\Delta tdk\Delta BT4295::BT4295}$ or *B.*
558 *theta*$^{\Delta tdk\Delta BT4295::\mathrm{T548S}}$ for ~2 weeks, following which all mice were adoptively transferred with a mix
559 of naïve BθOM CD45.1+CD45.2- CD4+ T cells and bulk wild-type CD45.1-CD45.2+ CD4+ T
560 cells (**Fig 6A**). ~3 weeks post transfer, the accumulation of BθOM CD4+ T cells was assessed in
561 the spleen and colon (**Fig S2**). BθOM CD4+ T cells were massively impaired in their capacity to
562 expand in mice colonized with *B. theta*$^{\Delta tdk\Delta BT4295::\mathrm{T548S}}$, both in terms of proportion of the colonic
563 (**Fig 6B and 6C**) and splenic (**Fig 6D**) CD4+ T cell pool as well as the total number of BθOM
564 cells that accumulated in the colon (**Fig 6E**), relative to mice colonized with the control *B.*
565 *theta*$^{\Delta tdk\Delta BT4295::BT4295}$ that expressed the wild-type form of the epitope. Indeed, the numbers of
566 BθOM CD4+ T cells were so low that accurate phenotyping of their differentiation profile was not
567 possible. No differences were observed in colonization capacity between the two strains (**Fig**
568 **6F**) suggesting that impaired colonization does not contribute to this phenotype. The total
569 number of CD4+ T cells that accumulated in the colon was also not significantly different
570 between the two groups (**Fig 6G**), suggesting that the impairment in BθOM CD4+ T cells was a
571 specific effect and not simply a more generalized feature that also affected BθOM CD4+ T cell
572 reconstitution. Thus, despite the fact that it can stimulate BθOM CD4+ T cells *in vitro*, the T548S
573 form of the epitope that is expressed in *B. theta*-dnLKV9 is also not sufficient to restore its
574 capacity to stimulate the accumulation of BθOM CD4+ T cells in the intestine, likely because it
575 does not provide adequate signal through the TCR at the doses available *in vivo*.

576

577

578

579

580

581

582

583 **Discussion**

584 Here we investigated whether a species-specific CD4+ T cell clone, as represented by CD4+ T
585 cells from BθOM TCR transgenic mice, could uniformly respond to multiple members of the
586 *Bacteroides thetaiotaomicron* species or if particular strains could evade recognition. We found
587 that while many tested strains were recognized by BθOM CD4+ T cells leading to their activation
588 equivalent to the type strain *B. theta*-VPI-5482, one strain, *B. theta*-dnLKV9, was severely
589 impaired in its capacity to activate these cells, both *in vitro* and *in vivo* in gnotobiotic mice.
590 Importantly, this evasion of recognition could not simply be attributed to a lack of the gene
591 encoding the activating epitope, *BT4295*. We identified that *B. theta*-dnLKV9 harbored a
592 premature stop codon within its homolog of *BT4295* that was downstream of the epitope, and by
593 reconstructing this mutation in *B. theta*-VPI-5482 that lacked its own copy of *BT4295*, showed
594 that this mutation was sufficient to ablate recognition, thus conferring evasion of BθOM CD4+ T
595 cells to a permissive strain. We further identified an additional homolog of *BT4295* that was
596 present in *B. theta*-dnLKV9 but not *B. theta*-VPI-5482. This copy harbored an altered version of
597 the epitope, with a T548S amino acid substitution that led to a significant reduction in the
598 capacity to stimulate BθOM CD4+ T cells both *in vitro* and *in vivo* in gnotobiotic mice. Thus, our
599 data uncover strain-specific modifications to an immunodominant CD4+ T cell antigen in *B.*
600 *theta* that facilitate evasion of recognition by select CD4+ T cells. Our data point to mechanisms
601 through which individual strains can evade recognition of T cell clones directed against antigens
602 they express and point to a mechanism through which individualized pools of CD4+ T cells for
603 strains can develop. Such a tailored response could explain how intestinal CD4+ T cells avoid
604 inappropriate and damaging responses directed towards symbionts that have been generated in
605 response to pathogenic isolates with the same epitope.

606 Several TCR transgenic mice have now been developed that are specific for microbiome-
607 encoded epitopes [19, 26, 27, 30, 32, 68, 69]. These tools have provided pivotal insights into
608 modulation of CD4+ T cell function by the microbiome, revealing that microbiome-specific CD4+
609 T cells can adopt a variety of cell fates following recognition [19, 20, 26, 27, 30, 32, 68], that
610 vary depending both on the specific microbe that expresses the antigen [27], the presence or
611 absence of inflammation [26, 30, 32, 70], and the nature of the other community members
612 present [19, 48]. Despite these advances, it has remained largely unclear whether the observed
613 responses are representative of the target species as a whole, or if strain-level variation exists,
614 a feature of many interactions between hosts and pathogens that has only begun to be explored
615 for microbiome-driven immune phenotypes [41-43, 45, 71-77]. Our studies suggest that while a
616 given T cell clone may be responsive to many strains of a species, it cannot be assumed that a
617 TCR of known specificity will respond to a microbe where this has not been empirically tested,
618 even when the strains express the target epitope of interest. Together with an emerging body of
619 work, our data suggest that strain-level variation is an important feature with respect to immune
620 modulation by the microbiome that warrants more detailed study. Although it is important to
621 highlight that the use of RAG-deficient and gnotobiotic mice can lead to greater activation of
622 adoptively transferred microbiome-specific T cells than would be observed in more "natural"
623 environments [48, 78], this provided the greatest opportunity for *B. theta*-dnLKV9 to activate
624 BθOM CD4+ T cells, and thus any defects observed here are likely to be magnified in the
625 context of lymphocyte replete hosts and/or mice born with complex microbiomes.

626 Prior studies have revealed the capacity of CD4+ T cell clones to respond to phylogenetically
627 related microbes that share the target epitope, or even to modified forms of the epitope,

628 providing a mechanism through which a broad array of microbes could be recognized by a
629 single T cell clone [28, 29, 40]. More recently, it has been shown that the most abundant TCRs
630 in the intestinal CD4+ T cell compartment react to microbiome-derived epitopes that are widely
631 shared and highly expressed [40]. This model provides an explanation for how a limited number
632 of CD4+ T cell clones can react to a broad array of microbes through focusing of the TCR
633 repertoire on broadly and highly expressed antigens, supporting a notion of community-level
634 epitope immunodominance. However, the model does not account for the need to tailor the
635 immune response at the strain-level, due to the capacity of closely related strains to have
636 opposing impact on host health [41-47]. Studies tracking the fate of an antigen from SFB have
637 shown that when expressed in SFB, TCR transgenic cells specific for the target SFB-derived
638 antigen adopt a Th17 fate in the intestine, but when the same antigen is expressed in *Listeria*
639 *monocytogenes*, the cells adopt a Th1 fate [27]. Although this involved forced expression of an
640 epitope that was not truly shared between SFB and *L. monocytogenes*, it demonstrated that
641 distinct fates can be primed against the same epitope in the intestine, underscoring the need for
642 responses to be tailored to the nature of the microbe from which they are derived rather than a
643 uniform response irrespective of the impact of the source of the epitope on the host. Our data
644 suggest that even if deleterious responses are primed against a shared epitope, individual
645 strains that express the epitope may evolve strategies to evade recognition, or indeed simply
646 acquire random mutations, that limit the activity of particular T cell clones against them.
647 Collectively, these data add to the current model through which the regulation of intestinal CD4+
648 T cell responses is conceptualized, providing insights into how a CD4+ T cell compartment of a
649 limited size balances the need for broad reactivity with the fine-level specificity needed to tailor
650 responses in a strain-specific manner. Although much work remains to be done, we posit that for
651 each individual strain the quality of the response will be dictated by the collective function of all
652 the CD4+ T cells that recognize the strain, thus allowing a highly individualized output even
653 where some of the clones within the pool have been polarized by a different strain. Under such
654 a scenario, we envision that a collection of "public" T cell clones exist that are specific for a large
655 number of community members that share an epitope in addition to "private" T cell clones that
656 are highly strain-specific. Thus, for a commensal microbiome member with a closely related
657 pathogen/pathobiont, T cell clones with inflammatory potential that are elicited by the pathogenic
658 agent may also react to the commensal, but ultimately, the existence of sufficient anti-
659 commensal T cell clones with anti-inflammatory potential will invoke tolerance to the commensal
660 while allowing the function of protective inflammatory functions where necessary. Although it is
661 clear that many other factors will contribute to the maintenance of immune tolerance, we
662 hypothesize that this forms one of the layers of mutualism that limits deleterious anti-
663 microbiome T cell responses in the intestine.

664 Although our data only provides evidence of evasion of a single TCR clone by one strain of
665 bacteria, additional evidence for this phenomenon has been provided in a prior study of a
666 distinct *B. theta*-reactive TCR [28]. Using a hybridoma-based approach, an epitope within
667 BT0900 of *B. theta*-VPI-5482 was found to be shared with other *Bacteroides* species,
668 specifically *B. finegoldii*, *B. ovatus*, and *B. caccae*, with a 100% match in epitope sequence
669 across the different species. However, although both *B. finegoldii* and *B. ovatus* could activate
670 this hybridoma, *B. caccae* lacked any capacity to do so above that of a *BT0900*-deletion mutant.
671 While the mechanisms involved are undefined, these data reveal that evasion of individual
672 CD4+ T cell clones, even when carrying an exact epitope match, is not simply a feature of *B.*
673 *theta*-dnLKV9 and may represent a common feature among gut microbes.

674 Finally, our study identified the existence of a naturally occurring altered peptide ligand (APL) in
675 an immunodominant epitope, represented by a T548S substitution in the epitope recognized by
676 the *B. theta*-specific BθOM TCR. APLs have long been recognized as a means through which
677 the strength of TCR stimulation and the quality of the ensuing response can be modulated [57,
678 58, 79-84]. As such, they have provided a means through which pathogens can disarm host-
679 protective T cell responses, by antagonizing the TCR or altering the quality of the response [79-
680 82]. As only a handful of microbiome-derived CD4+ T cell epitopes have been defined [26-29],
681 and often few isolates of a species have complete genome sequences available, the prevalence
682 of APLs in the gut microbiome has not been studied in detail, although the existence of altered
683 epitopes that impaired recognition have been previously identified [29]. The APL identified here
684 (EEFNLPTSNGGHAT) has weak stimulatory power *in vitro* and did not appear to limit the
685 stimulation when mixed with the native form of the epitope (EEFNLPTTNGGHAT), suggesting
686 that it lacks the inhibitory capacity of many APLs [58, 85]. As naturally occurring APL of a
687 flagellin-derived peptide from *Salmonella* stimulate lower production of interferon-γ from
688 flagellin-specific SM1 cells relative to the native epitope [84] we were interested to determine if
689 the T548S APL would skew the balance of different effector fates. In the intestine, BθOM CD4+
690 T cells adopt a FoxP3+ Treg fate as well as pro-inflammatory cytokine secreting potential that is
691 limited by the developing Tregs [32]. However, as the T548S APL did not lead to appreciable
692 accumulation of BθOM CD4+ T cells *in vivo*, we were unable to determine if this modulation
693 shaped phenotypic effector outcomes.

694 Although our data do not provide a means through which the prevalence of such APL can be
695 estimated, they suggest that such alterations may play an important role in shaping CD4+ T cell
696 responses against individual strains in the gut. While it is tempting to speculate that the APL
697 represents a means of escaping CD4+ T cell recognition in general, this cannot be reliably
698 ascertained from our data. The BθOM TCR was isolated from popliteal lymph node CD4+ T
699 cells from mice that had been immunized with *B. theta*-VPI-5482, and it is possible that the
700 T548S version is equally immunogenic and would be the target of a strong CD4+ T cell
701 response in the context of colonization/immunization with *B. theta*-dnLKV9. Indeed, *B. theta*-
702 VPI-5482 may escape recognition by such cells directed against *B. theta*-dnLKV9. However,
703 irrespective of whether the T548S APL represents an immune evasion strategy, or whether it
704 simply represents an equally immunogenic variant recognized by a distinct T cell clone, our data
705 show that *B. theta*-dnLKV9 can evade recognition by a CD4+ T cell clone that recognizes a
706 wide-array of other *B. theta* strains. Thus, while it is likely that numerous CD4+ T cell clones that
707 emerge following colonization with *B. theta*-dnLKV9 or *B. theta*-VPI-5482 would be strongly
708 reactive to both strains, this is not a uniform process. Indeed, prior work has shown that the
709 expression of *BT4295*, which encodes the epitope recognized by BθOM CD4+ T cells, is
710 sensitive to dietary components [32], reinforcing the existence of myriad mechanisms through
711 which recognition can be evaded. These data also highlight T548 as an important residue for
712 BθOM CD4+ T cell recognition of the epitope, adding to previous findings that showed that T547
713 is a critical residue within the epitope [32]. Our work now extends our knowledge of the critical
714 determinants within the epitope, and further reveals how it may represent a site whose
715 modification can enhance or ablate recognition depending on the specific substitution.

716 Collectively, our data show that CD4+ T cells should be considered as strain-specific and
717 suggest the existence of public and private responses that balance to provide broad reactivity
718 that maintains the strain-level discrimination needed to ensure the appropriate response is

mounted against the numerous microbial strains resident in the gut microbiome. This adds to a growing body of work defining how immunity to *Bacteroides thetaiotaomicron* is mediated in steady state and disease [15, 18, 31, 32, 49, 56, 86], and underscores the need to study strain-level variation in gut microorganisms.

Acknowledgments

We are indebted to the members of the Gnotobiotic Core facility at the Lerner Research Institute, especially Brandon Bakos, for help with execution of gnotobiotic experiments. We are extremely grateful to Prof. Thaddeus Stappenbeck for kindly providing us the *B. thetaiotaomicron*-dnLKV9 strain, Prof. Eric Martens for the provision of *BT4295* deficient *B. thetaiotaomicron*, Prof. Paul Allen for the provision of BθOM mice, Stephen Horvath and Darren Kreamalmeyer for advice regarding genotyping and breeding of BθOM mice, and Prof. Andrew Kau, Prof. Meng Wu and Dr. John Dekker for insightful comments on these studies.

Author Contributions

R.W.P.G. designed and executed all experiments relating to the evasion of BθOM CD4+ T cells by various strains of *B. thetaiotaomicron*, generated the described genetically modified forms of *B. thetaiotaomicron*, analyzed and interpreted data, and helped write the manuscript. J.M.T., O.D.B., and M.J.E. assisted with the described experiments, and provided input on data interpretation. P.P.A. helped to design the described experiments, interpret and analyze data, and helped to write the manuscript.

Financial Support

R.W.P.G. is the recipient of NIH Loan Repayment Awards: LRP0000016021 and LRP0000045724. This work was supported by funds from the Cleveland Clinic and R01DK126772 from the National Institute of Diabetes and Digestive and Kidney Diseases Foundation awarded to the lab of P.P.A.

Conflicts

The authors do not have any financial conflicts of interest to declare.

785 **References**

786 1. Honda, K. and D.R. Littman, *The microbiome in infectious disease and inflammation.*
787 Annu Rev Immunol, 2012. **30**: p. 759-95.
788 2. Ost, K.S. and J.L. Round, *Communication Between the Microbiota and Mammalian*
789 *Immunity.* Annu Rev Microbiol, 2018. **72**: p. 399-422.
790 3. Hooper, L.V., T. Midtvedt, and J.I. Gordon, *How host-microbial interactions shape the*
791 *nutrient environment of the mammalian intestine.* Annu Rev Nutr, 2002. **22**: p. 283-307.
792 4. Ahern, P.P. and K.J. Maloy, *Understanding immune-microbiota interactions in the*
793 *intestine.* Immunology, 2020. **159**(1): p. 4-14.
794 5. Smith, K., K.D. McCoy, and A.J. Macpherson, *Use of axenic animals in studying the*
795 *adaptation of mammals to their commensal intestinal microbiota.* Semin Immunol, 2007.
796 **19**(2): p. 59-69.
797 6. Geuking, M.B. and R. Burkhard, *Microbial modulation of intestinal T helper cell*
798 *responses and implications for disease and therapy.* Mucosal Immunol, 2020. **13**(6): p.
799 855-866.
800 7. Honda, K. and D.R. Littman, *The microbiota in adaptive immune homeostasis and*
801 *disease.* Nature, 2016. **535**(7610): p. 75-84.
802 8. Ivanov, II, et al., *T Cell Responses to the Microbiota.* Annu Rev Immunol, 2022. **40**: p.
803 559-587.
804 9. Gaboriau-Routhiau, V., et al., *The key role of segmented filamentous bacteria in the*
805 *coordinated maturation of gut helper T cell responses.* Immunity, 2009. **31**(4): p. 677-89.
806 10. Ivanov, II, et al., *Induction of intestinal Th17 cells by segmented filamentous bacteria.*
807 Cell, 2009. **139**(3): p. 485-98.
808 11. Ivanov, II, et al., *Specific microbiota direct the differentiation of IL-17-producing T-helper*
809 *cells in the mucosa of the small intestine.* Cell Host Microbe, 2008. **4**(4): p. 337-49.
810 12. Tan, T.G., et al., *Identifying species of symbiont bacteria from the human gut that, alone,*
811 *can induce intestinal Th17 cells in mice.* Proc Natl Acad Sci U S A, 2016. **113**(50): p.
812 E8141-E8150.
813 13. Atarashi, K., et al., *Treg induction by a rationally selected mixture of Clostridia strains*
814 *from the human microbiota.* Nature, 2013. **500**(7461): p. 232-6.
815 14. Atarashi, K., et al., *Induction of colonic regulatory T cells by indigenous Clostridium*
816 *species.* Science, 2011. **331**(6015): p. 337-41.
817 15. Faith, J.J., et al., *Identifying gut microbe-host phenotype relationships using*
818 *combinatorial communities in gnotobiotic mice.* Sci Transl Med, 2014. **6**(220): p.
819 220ra11.
820 16. Geuking, M.B., et al., *Intestinal bacterial colonization induces mutualistic regulatory T*
821 *cell responses.* Immunity, 2011. **34**(5): p. 794-806.
822 17. Ohnmacht, C., et al., *MUCOSAL IMMUNOLOGY. The microbiota regulates type 2*
823 *immunity through RORgammat(+) T cells.* Science, 2015. **349**(6251): p. 989-93.
824 18. Sefik, E., et al., *MUCOSAL IMMUNOLOGY. Individual intestinal symbionts induce a*
825 *distinct population of RORgamma(+) regulatory T cells.* Science, 2015. **349**(6251): p.
826 993-7.
827 19. Ansaldo, E., et al., *Akkermansia muciniphila induces intestinal adaptive immune*
828 *responses during homeostasis.* Science, 2019. **364**(6446): p. 1179-1184.
829 20. Overacre-Delgoffe, A.E., et al., *Microbiota-specific T follicular helper cells drive tertiary*
830 *lymphoid structures and anti-tumor immunity against colorectal cancer.* Immunity, 2021.
831 **54**(12): p. 2812-2824 e4.
832 21. Furusawa, Y., et al., *Commensal microbe-derived butyrate induces the differentiation of*
833 *colonic regulatory T cells.* Nature, 2013. **504**(7480): p. 446-50.

22. Geem, D., et al., *Specific microbiota-induced intestinal Th17 differentiation requires MHC class II but not GALT and mesenteric lymph nodes.* J Immunol, 2014. **193**(1): p. 431-8.
23. Lochner, M., et al., *Restricted microbiota and absence of cognate TCR antigen leads to an unbalanced generation of Th17 cells.* J Immunol, 2011. **186**(3): p. 1531-7.
24. Goto, Y., et al., *Segmented filamentous bacteria antigens presented by intestinal dendritic cells drive mucosal Th17 cell differentiation.* Immunity, 2014. **40**(4): p. 594-607.
25. Kullberg, M.C., et al., *Bacteria-triggered CD4(+) T regulatory cells suppress Helicobacter hepaticus-induced colitis.* J Exp Med, 2002. **196**(4): p. 505-15.
26. Xu, M., et al., *c-MAF-dependent regulatory T cells mediate immunological tolerance to a gut pathobiont.* Nature, 2018. **554**(7692): p. 373-377.
27. Yang, Y., et al., *Focused specificity of intestinal TH17 cells towards commensal bacterial antigens.* Nature, 2014. **510**(7503): p. 152-6.
28. Perez-Munoz, M.E., et al., *Identification and Phylogeny of the First T Cell Epitope Identified from a Human Gut Bacteroides Species.* PLoS One, 2015. **10**(12): p. e0144382.
29. Kullberg, M.C., et al., *Induction of colitis by a CD4+ T cell clone specific for a bacterial epitope.* Proc Natl Acad Sci U S A, 2003. **100**(26): p. 15830-5.
30. Chai, J.N., et al., *Helicobacter species are potent drivers of colonic T cell responses in homeostasis and inflammation.* Sci Immunol, 2017. **2**(13).
31. Hickey, C.A., et al., *Colitogenic Bacteroides thetaiotaomicron Antigens Access Host Immune Cells in a Sulfatase-Dependent Manner via Outer Membrane Vesicles.* Cell Host Microbe, 2015. **17**(5): p. 672-80.
32. Wegorzewska, M.M., et al., *Diet modulates colonic T cell responses by regulating the expression of a Bacteroides thetaiotaomicron antigen.* Sci Immunol, 2019. **4**(32).
33. Cebula, A., et al., *Thymus-derived regulatory T cells contribute to tolerance to commensal microbiota.* Nature, 2013. **497**(7448): p. 258-62.
34. Lathrop, S.K., et al., *Peripheral education of the immune system by colonic commensal microbiota.* Nature, 2011. **478**(7368): p. 250-4.
35. Hegazy, A.N., et al., *Circulating and Tissue-Resident CD4(+) T Cells With Reactivity to Intestinal Microbiota Are Abundant in Healthy Individuals and Function Is Altered During Inflammation.* Gastroenterology, 2017. **153**(5): p. 1320-1337 e16.
36. Kuczma, M.P., et al., *Commensal epitopes drive differentiation of colonic T(regs).* Sci Adv, 2020. **6**(16): p. eaaz3186.
37. Nutsch, K., et al., *Rapid and Efficient Generation of Regulatory T Cells to Commensal Antigens in the Periphery.* Cell Rep, 2016. **17**(1): p. 206-220.
38. Sercarz, E.E., et al., *Dominance and crypticity of T cell antigenic determinants.* Annu Rev Immunol, 1993. **11**: p. 729-66.
39. Mason, D., *A very high level of crossreactivity is an essential feature of the T-cell receptor.* Immunol Today, 1998. **19**(9): p. 395-404.
40. Nagashima, K., et al., *Mapping the T cell repertoire to a complex gut bacterial community.* Nature, 2023. **621**(7977): p. 162-170.
41. Chung, L., et al., *Bacteroides fragilis Toxin Coordinates a Pro-carcinogenic Inflammatory Cascade via Targeting of Colonic Epithelial Cells.* Cell Host Microbe, 2018. **23**(2): p. 203-214 e5.
42. Rhee, K.J., et al., *Induction of persistent colitis by a human commensal, enterotoxigenic Bacteroides fragilis, in wild-type C57BL/6 mice.* Infect Immun, 2009. **77**(4): p. 1708-18.
43. Wu, S., et al., *A human colonic commensal promotes colon tumorigenesis via activation of T helper type 17 T cell responses.* Nat Med, 2009. **15**(9): p. 1016-22.
44. Carrow, H.C., L.E. Batachari, and H. Chu, *Strain diversity in the microbiome: Lessons from Bacteroides fragilis.* PLoS Pathog, 2020. **16**(12): p. e1009056.

45. Wagner, V.E., et al., *Effects of a gut pathobiont in a gnotobiotic mouse model of childhood undernutrition.* Sci Transl Med, 2016. **8**(366): p. 366ra164.
46. Brenner, D.J., et al., *Polynucleotide sequence relatedness among three groups of pathogenic Escherichia coli strains.* Infect Immun, 1972. **6**(3): p. 308-15.
47. Pupo, G.M., R. Lan, and P.R. Reeves, *Multiple independent origins of Shigella clones of Escherichia coli and convergent evolution of many of their characteristics.* Proc Natl Acad Sci U S A, 2000. **97**(19): p. 10567-72.
48. Hoces, D., et al., *Microbiota colonization tunes the antigen threshold of microbiota-specific T cell activation in the gut.* bioRxiv, 2022: p. 2022.07.29.501979.
49. Engelhart, M.J., et al., *The NQR Complex Regulates the Immunomodulatory Function of Bacteroides thetaiotaomicron.* J Immunol, 2023. **211**(5): p. 767-781.
50. Rogers, T.E., et al., *Dynamic responses of Bacteroides thetaiotaomicron during growth on glycan mixtures.* Mol Microbiol, 2013. **88**(5): p. 876-90.
51. Glowacki, R.W.P., et al., *A Ribose-Scavenging System Confers Colonization Fitness on the Human Gut Symbiont Bacteroides thetaiotaomicron in a Diet-Specific Manner.* Cell Host Microbe, 2020. **27**(1): p. 79-92 e9.
52. Altschul, S.F., et al., *Basic local alignment search tool.* J Mol Biol, 1990. **215**(3): p. 403-10.
53. Edgar, R.C., *MUSCLE: a multiple sequence alignment method with reduced time and space complexity.* BMC Bioinformatics, 2004. **5**: p. 113.
54. Yamashita, I., et al., *CD69 cell surface expression identifies developing thymocytes which audition for T cell antigen receptor-mediated positive selection.* Int Immunol, 1993. **5**(9): p. 1139-50.
55. Testi, R., J.H. Phillips, and L.L. Lanier, *Leu 23 induction as an early marker of functional CD3/T cell antigen receptor triggering. Requirement for receptor cross-linking, prolonged elevation of intracellular [Ca++] and stimulation of protein kinase C.* J Immunol, 1989. **142**(6): p. 1854-60.
56. Bloom, S.M., et al., *Commensal Bacteroides species induce colitis in host-genotype-specific fashion in a mouse model of inflammatory bowel disease.* Cell Host Microbe, 2011. **9**(5): p. 390-403.
57. Evavold, B.D. and P.M. Allen, *Separation of IL-4 production from Th cell proliferation by an altered T cell receptor ligand.* Science, 1991. **252**(5010): p. 1308-10.
58. Sloan-Lancaster, J., B.D. Evavold, and P.M. Allen, *Induction of T-cell anergy by altered T-cell-receptor ligand on live antigen-presenting cells.* Nature, 1993. **363**(6425): p. 156-9.
59. Malherbe, L., et al., *Clonal selection of helper T cells is determined by an affinity threshold with no further skewing of TCR binding properties.* Immunity, 2004. **21**(5): p. 669-79.
60. Leitenberg, D., et al., *CD4 regulation of TCR signaling and T cell differentiation following stimulation with peptides of different affinities for the TCR.* J Immunol, 1998. **161**(3): p. 1194-203.
61. Brogdon, J.L., D. Leitenberg, and K. Bottomly, *The potency of TCR signaling differentially regulates NFATc/p activity and early IL-4 transcription in naive CD4+ T cells.* J Immunol, 2002. **168**(8): p. 3825-32.
62. Fasso, M., et al., *T cell receptor (TCR)-mediated repertoire selection and loss of TCR vbeta diversity during the initiation of a CD4(+) T cell response in vivo.* J Exp Med, 2000. **192**(12): p. 1719-30.
63. Corse, E., R.A. Gottschalk, and J.P. Allison, *Strength of TCR-peptide/MHC interactions and in vivo T cell responses.* J Immunol, 2011. **186**(9): p. 5039-45.
64. Corse, E., et al., *Attenuated T cell responses to a high-potency ligand in vivo.* PLoS Biol, 2010. **8**(9).

935 65. Ploquin, M.J., U. Eksmond, and G. Kassiotis, *B cells and TCR avidity determine distinct*
936 *functions of CD4+ T cells in retroviral infection.* J Immunol, 2011. **187**(6): p. 3321-30.
937 66. Keck, S., et al., *Antigen affinity and antigen dose exert distinct influences on CD4 T-cell*
938 *differentiation.* Proc Natl Acad Sci U S A, 2014. **111**(41): p. 14852-7.
939 67. Kunzli, M., et al., *Opposing effects of T cell receptor signal strength on CD4 T cells*
940 *responding to acute versus chronic viral infection.* Elife, 2021. **10**.
941 68. Cong, Y., et al., *A dominant, coordinated T regulatory cell-IgA response to the intestinal*
942 *microbiota.* Proc Natl Acad Sci U S A, 2009. **106**(46): p. 19256-61.
943 69. Harrison, O.J., et al., *Commensal-specific T cell plasticity promotes rapid tissue*
944 *adaptation to injury.* Science, 2019. **363**(6422).
945 70. Hand, T.W., et al., *Acute gastrointestinal infection induces long-lived microbiota-specific*
946 *T cell responses.* Science, 2012. **337**(6101): p. 1553-6.
947 71. Yang, C., et al., *Fecal IgA Levels Are Determined by Strain-Level Differences in*
948 *Bacteroides ovatus and Are Modifiable by Gut Microbiota Manipulation.* Cell Host
949 Microbe, 2020. **27**(3): p. 467-475 e6.
950 72. Carvalho, F.A., et al., *Crohn's disease adherent-invasive Escherichia coli colonize and*
951 *induce strong gut inflammation in transgenic mice expressing human CEACAM.* J Exp
952 Med, 2009. **206**(10): p. 2179-89.
953 73. Mazmanian, S.K., J.L. Round, and D.L. Kasper, *A microbial symbiosis factor prevents*
954 *intestinal inflammatory disease.* Nature, 2008. **453**(7195): p. 620-5.
955 74. Round, J.L. and S.K. Mazmanian, *Inducible Foxp3+ regulatory T-cell development by a*
956 *commensal bacterium of the intestinal microbiota.* Proc Natl Acad Sci U S A, 2010.
957 **107**(27): p. 12204-9.
958 75. Viladomiu, M., et al., *IgA-coated E. coli enriched in Crohn's disease spondyloarthritis*
959 *promote T(H)17-dependent inflammation.* Sci Transl Med, 2017. **9**(376).
960 76. Arthur, J.C., et al., *Intestinal inflammation targets cancer-inducing activity of the*
961 *microbiota.* Science, 2012. **338**(6103): p. 120-3.
962 77. Round, J.L., et al., *The Toll-like receptor 2 pathway establishes colonization by a*
963 *commensal of the human microbiota.* Science, 2011. **332**(6032): p. 974-7.
964 78. Kwong Chung, C.K., F. Ronchi, and M.B. Geuking, *Detrimental effect of systemic*
965 *antimicrobial CD4(+) T-cell reactivity on gut epithelial integrity.* Immunology, 2017.
966 **150**(2): p. 221-235.
967 79. Alleva, D.G., et al., *Immunological characterization and therapeutic activity of an altered-*
968 *peptide ligand, NBI-6024, based on the immunodominant type 1 diabetes autoantigen*
969 *insulin B-chain (9-23) peptide.* Diabetes, 2002. **51**(7): p. 2126-34.
970 80. Windhagen, A., et al., *Modulation of cytokine patterns of human autoreactive T cell*
971 *clones by a single amino acid substitution of their peptide ligand.* Immunity, 1995. **2**(4):
972 p. 373-80.
973 81. Bertoletti, A., et al., *Natural variants of cytotoxic epitopes are T-cell receptor antagonists*
974 *for antiviral cytotoxic T cells.* Nature, 1994. **369**(6479): p. 407-10.
975 82. Klenerman, P., et al., *Cytotoxic T-cell activity antagonized by naturally occurring HIV-1*
976 *Gag variants.* Nature, 1994. **369**(6479): p. 403-7.
977 83. Evavold, B.D., et al., *Separation of T helper 1 clone cytolysis from proliferation and*
978 *lymphokine production using analog peptides.* J Immunol, 1993. **150**(8 Pt 1): p. 3131-40.
979 84. Johanns, T.M., et al., *Naturally occurring altered peptide ligands control Salmonella-*
980 *specific CD4+ T cell proliferation, IFN-gamma production, and protective potency.* J
981 Immunol, 2010. **184**(2): p. 869-76.
982 85. De Magistris, M.T., et al., *Antigen analog-major histocompatibility complexes act as*
983 *antagonists of the T cell receptor.* Cell, 1992. **68**(4): p. 625-34.

86. Pereira, G.V., et al., *Opposing diet, microbiome, and metabolite mechanisms regulate inflammatory bowel disease in a genetically susceptible host.* Cell Host Microbe, 2024. **32**(4): p. 527-542 e9.

Figures

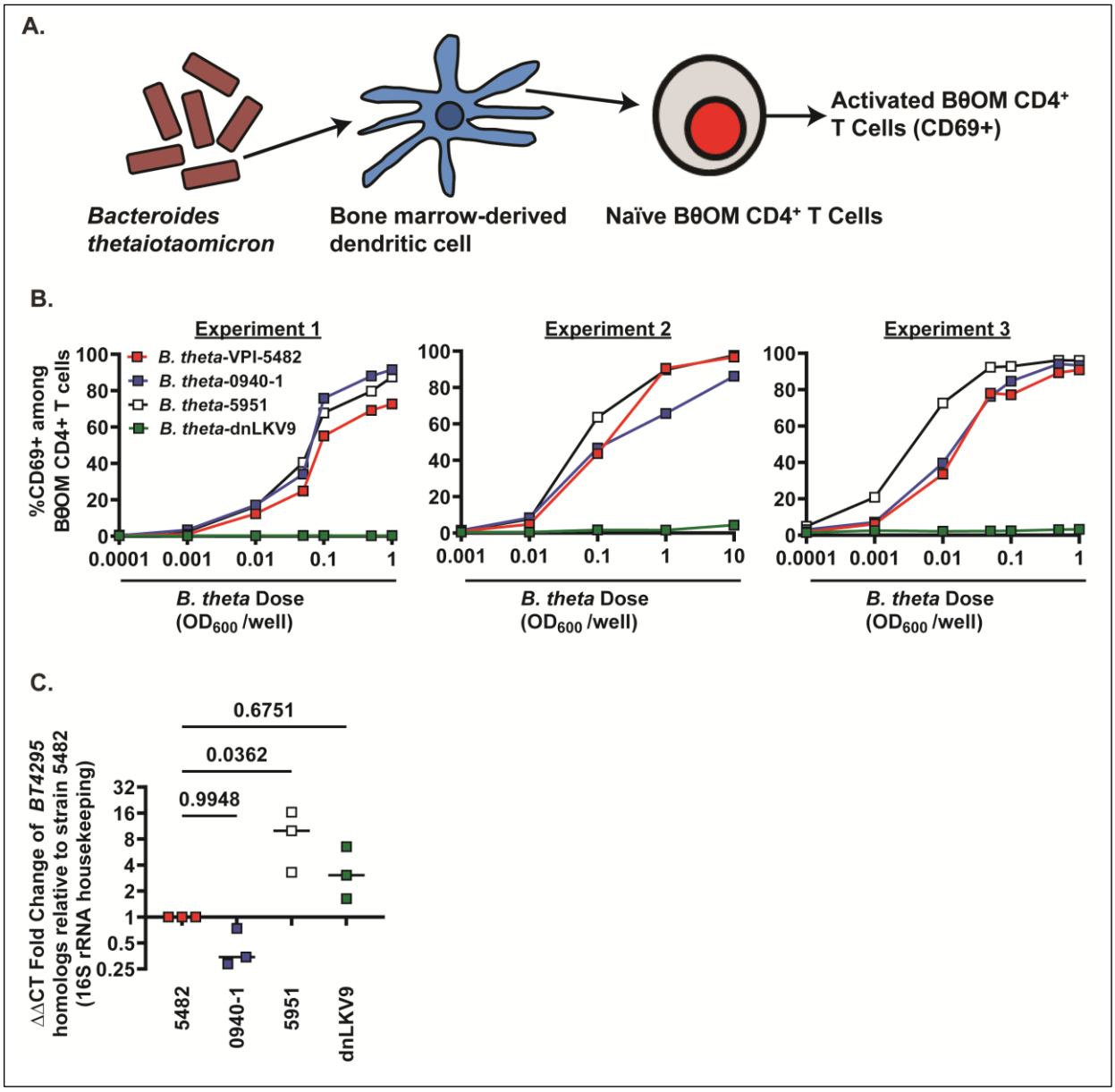
A.
Bacteroides thetaiotaomicron
Bone marrow-derived dendritic cell
Naïve BθOM CD4+ T Cells
Activated BθOM CD4+ T Cells (CD69+)
B.
Experiment 1
Experiment 2
Experiment 3
B. theta-VPI-5482
B. theta-0940-1
B. theta-5951
B. theta-dnLKV9
%CD69+ among BθOM CD4+ T cells
B. theta Dose (OD600 /well)
C.
0.6751
0.0362
0.9948
ΔΔCT Fold Change of BT4295 homologs relative to strain 5482 (16S rRNA housekeeping)
5482
0940-1
5951
dnLKV9

Figure 1-Select *B. theta* strains evade recognition by *B. thetaiotaomicron*-specific BθOM CD4+ T cells

(A) Schematic of experimental scheme to assess activation of BθOM CD4+ T cells by strains of *B. theta*.
(B) Bone-marrow derived dendritic cells were pre-loaded with the indicated doses of heat-killed strains of *B. thetaiotaomicron* for 24 hours and then mixed 1:1 with naïve BθOM CD4+ T cells. After 2 days CD69 expression was assessed by flow cytometry. Summary data of experiments described in (A) for the indicated strains of *B. theta.* Each data point represents a single technical replicate at the indicated dose, and three independent biological experiments are shown.
(C) The expression of *BT4295* or its relevant homologs in the indicated strains of *B. theta* was assessed at stationary phase, using the 16S rRNA gene as a housekeeping gene to calculate relative expression. The graph shows the fold change in expression relative to expression in *B. theta*-VPI-5482 as calculated by the ΔΔCt method. Bars show the median and each point represents an individual biological replicate. Statistical significance was determined via one-way ANOVA with Dunnett's multiple comparison test, comparisons made to *B. theta*-VPI-5482.

1045
1046
1047
1048
1049
1050
1051
1052
1053
1054
1055
1056
1057
1058
1059
1060
1061
1062

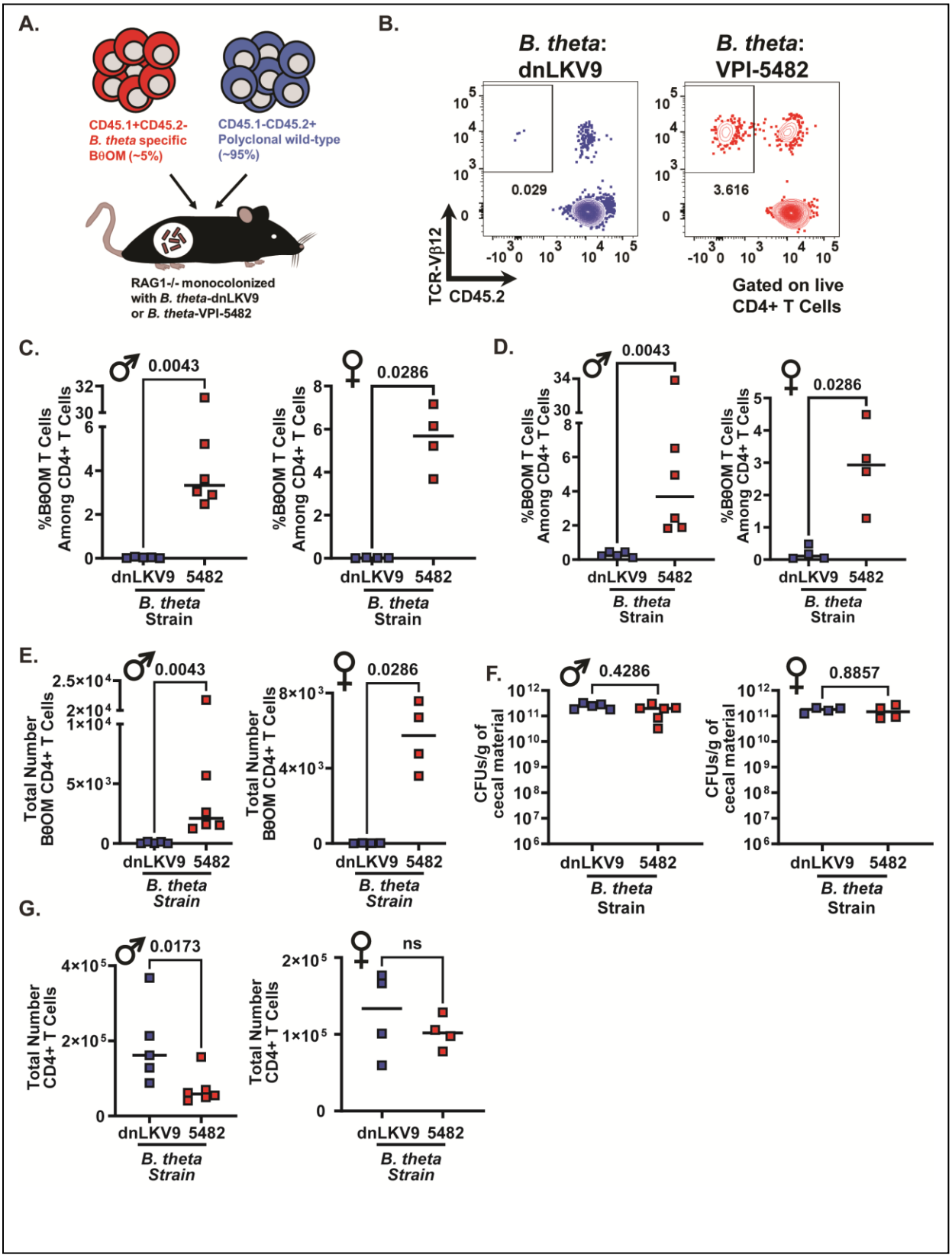
A.
CD45.1+CD45.2-
B. theta specific
BθOM (~5%)
CD45.1-CD45.2+
Polyclonal wild-type
(~95%)
RAG1-/- monocolonized
with B. theta-dnLKV9
or B. theta-VPI-5482
B.
B. theta:
dnLKV9
B. theta:
VPI-5482
0.029
3.616
TCR-Vβ12
CD45.2
Gated on live
CD4+ T Cells
C.
0.0043
0.0286
%BθOM T Cells
Among CD4+ T Cells
D.
0.0043
0.0286
%BθOM T Cells
Among CD4+ T Cells
dnLKV9
5482
B. theta
Strain
E.
0.0043
0.0286
Total Number
BθOM CD4+ T Cells
F.
0.4286
0.8857
CFUs/g of
cecal material
G.
0.0173
ns
Total Number
CD4+ T Cells

1063

Figure 2-*B. theta*-dnLKV9 evades recognition by BθOM CD4+ T cells *in vivo*

Naïve BθOM CD4+ T cells were mixed with unfractionated wild-type polyclonal CD4+ T cells and adoptively transferred to gnotobiotic RAG1-/- mice that had been colonized for ~2 weeks with the indicated strain of *B. theta*. ~3 weeks later the accumulation of BθOM CD4+ T cells was quantified

(A) Schematic outlining experimental design for cell transfer.
(B) Representative flow cytometry plots showing BθOM CD4+ T cell accumulation in the colon of the indicated groups of recipient mice (data shown is from male mice).
(C) Graph shows the proportion of BθOM CD4+ T cells among all CD4+ T cells in the colon for both male and female recipients ~3 weeks post cell transfer.
(D) Graph shows the proportion of BθOM CD4+ T cells among all CD4+ T cells in the spleen for both male and female recipients ~3 weeks post cell transfer.
(E) Graph shows the total number of BθOM CD4+ T cells in the colon of male and female recipients ~3 weeks post cell transfer.
(F) Graph shows the colonization levels of *B. theta* as quantified by enumeration of colony forming units (CFU) in the cecum ~5 weeks post colonization, ~3 weeks post cell transfer.
(G) Graph shows the total number of CD4+ T cells, encompassing BθOM and wild-type CD4+ T cells in the colon of both male and female recipient mice ~3 weeks post cell transfer.

Bars show the median and data points represent individual mice. Male and female cohorts represent two independent experiments. Statistical significance was determined via Mann-Whitney test. The data from one mouse was excluded from analysis due to technical issues during injection. The decision to exclude this data was taken at the time of injection prior to any knowledge of the outcome of the data. The exclusion of this data point did not affect conclusions drawn from the data. P values <0.05 were considered to be statistically significant. Symbols indicate the sex of the mice used: ♂ for male and ♀ for female.

1064

1065

1066

1067

1068

1069

1070

1071

1072

1073

1074

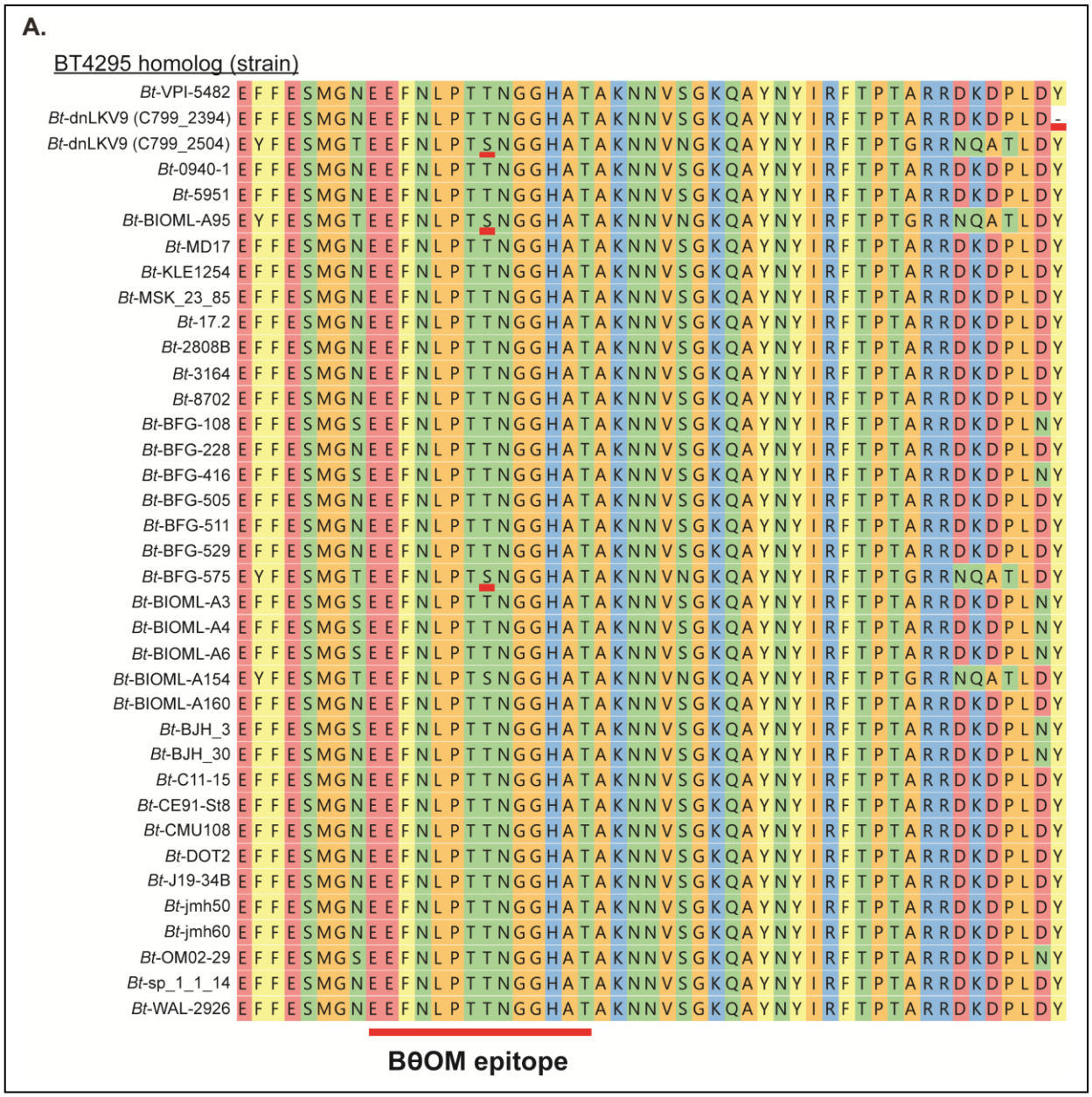

Figure 3-Bioinformatic analyses reveal variation in BT4295 across strains of *B. theta*

The amino acid sequence of BT4925 and its homologs from the indicated strains of *B. theta* was extracted from publicly available genome sequences and aligned to facilitate comparisons between the different strains. The illustration shows the region of BT4295 that contains the canonical form of the epitope recognized by BθOM CD4+ T cells and the region immediately downstream. The presence of an alteration in epitope sequence (T548S) for *B. theta*-dnLKV9 (C799_2504), *B. theta*-BIOML-A95 and *B. theta*-BFG-575 is underlined in red. The existence of a premature stop codon downstream of the epitope in *B. theta*-dnLKV9 (C799_2394) (marked as a "-"), but not other strains, is also highlighted in red. Note, *B. theta*-dnLKV9 (C799_2504) and *B. theta*-dnLKV9 (C799_2394) represent proteins encoded by two different homologs of *BT4295* in *B. theta*-dnLKV9.

1075

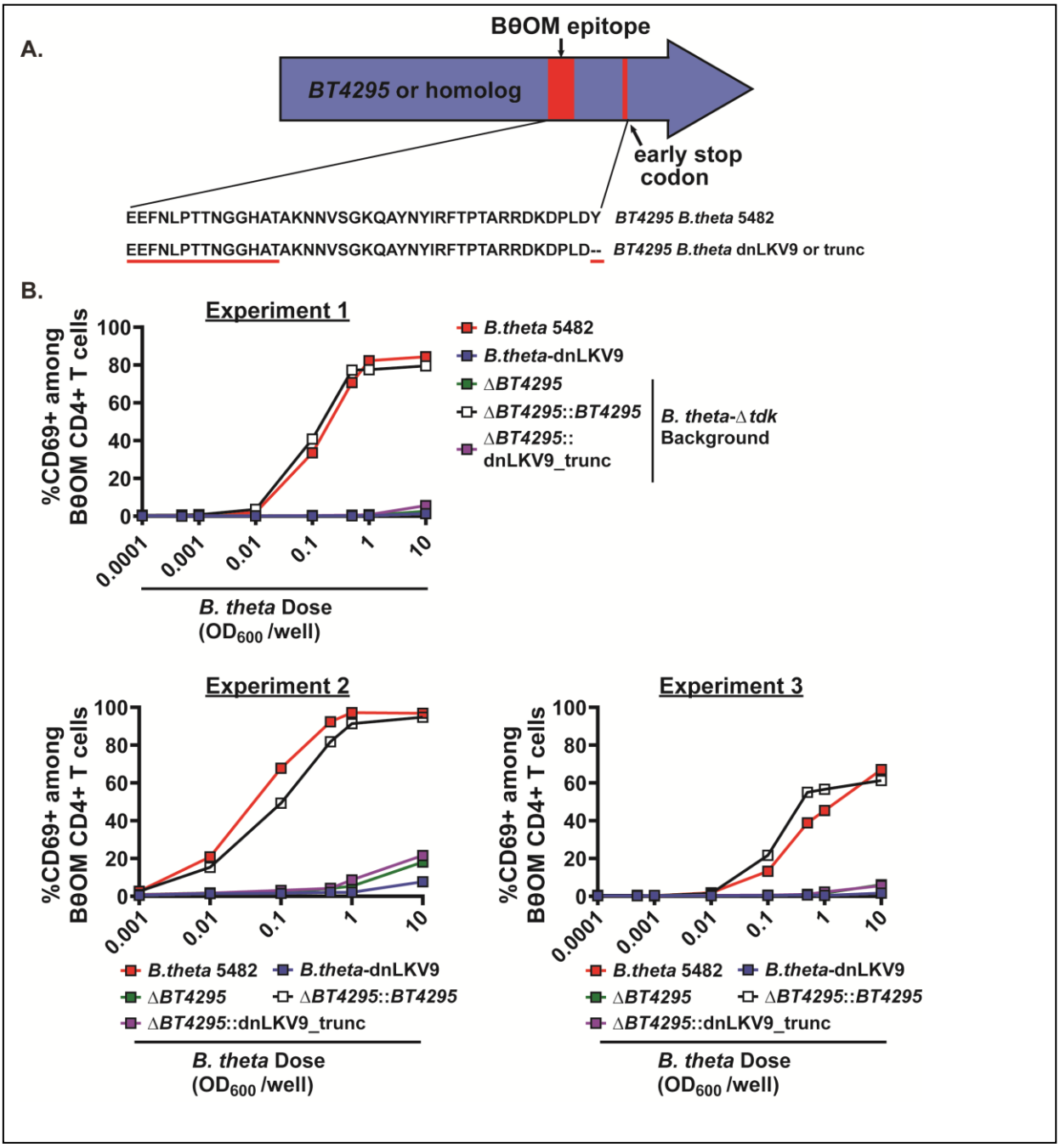

1076

1077

1078

1079

1080

1081

Figure 4-A premature stop codon within BT4295 ablates recognition by BθOM CD4+ T cells

(A) Schematic of a premature stop codon that was introduced into *B. theta*-VPI-5482$^{\Delta tdk \Delta BT4295}$ that mimicked that found in *B. theta*-dnLKV9 (*B. theta*-VPI-5482$^{\Delta tdk \Delta BT4295}$::dnLKV9_trunc). Note, all genetically modified strains were generated on a *B. theta*-VPI-5482$^{\Delta tdk \Delta BT4295}$ background.

(B) Bone-marrow derived dendritic cells were pre-loaded with varying doses of heat-killed *B. theta*-VPI-5482$^{\Delta tdk \Delta BT4295}$::dnLKV9_trunc or the indicated controls for 24 hours following which they were mixed 1:1 with naïve BθOM CD4+ T cells. After 2 days CD69 expression was assessed by flow cytometry. Each data point represents a single technical replicate at the indicated dose, and summary data for three independent biological experiments are shown.

1082

1083

1084

1085

1086

1087

1088

1089

1090

1091

1092

1093

1094

1095

1096

1097

1098

1099

1100

1101

1102

1103

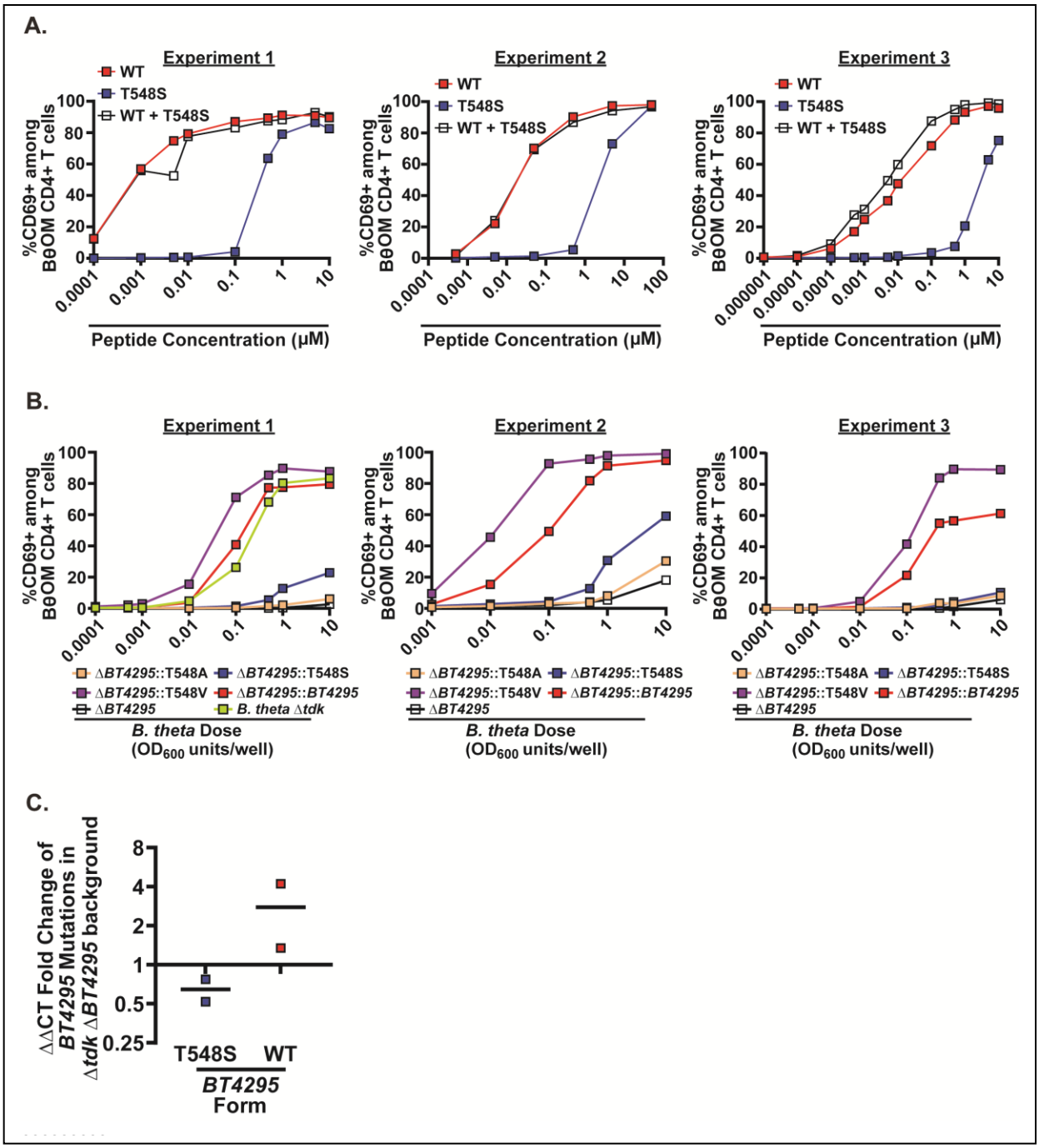
A.
Experiment 1
Experiment 2
Experiment 3
WT
T548S
WT + T548S
%CD69+ among BθOM CD4+ T cells
Peptide Concentration (μM)
B.
ΔBT4295::T548A
ΔBT4295::T548S
ΔBT4295::T548V
ΔBT4295::BT4295
ΔBT4295
B. theta Δtdk
B. theta Dose (OD600 units/well)
C.
ΔΔCT Fold Change of BT4295 Mutations in Δtdk ΔBT4295 background
T548S
WT
BT4295 Form

Figure 5-*B. theta*-dnLKV9 harbors an altered peptide ligand for BθOM CD4^{+} T cells with reduced potency

(A) Bone-marrow derived dendritic cells were loaded with varying doses of synthetic peptides representing the canonical form of the epitope for BθOM CD4+ T cells found in *B. theta*-VPI-5482, a mutated form of the epitope found in *B. theta*-dnLKV9 (T548S), or a mixture of both peptides, for 24 hours. Following this, the cells were mixed 1:1 with naïve BθOM CD4+ T cells and were incubated for 2 days. CD69 expression was then assessed by flow cytometry.

(B) Bone-marrow derived dendritic cells were loaded with varying doses of heat-killed *B. theta*-VPI-5482$^{\Delta tdk\Delta BT4295}$ that had been modified to express the indicated variants of the epitope recognized by BθOM CD4+ T cells. Following this, the cells were mixed 1:1 with naïve BθOM CD4+ T cells and were incubated for 2 days. CD69 expression was then assessed by flow cytometry.

(C) The expression of *BT4295* forms in *B. theta*$^{\Delta tdk\Delta BT4295::BT4295}$ (WT) *or B. theta*$^{\Delta tdk\Delta BT4295::T548s}$ (T548S) was assessed at stationary phase, using the 16S rRNA gene as a housekeeping gene to calculate relative expression. The graph shows the fold change in expression relative to expression in *B. theta*-VPI-5482 as calculated by the ΔΔCt method. This analysis was performed concurrently with the data in Figure 1C, and thus the expression in *B. theta*-VPI-5482 used for normalization is the same for both graphs.

Each point represents a single technical replicate at the indicated dose, (A) and (B). The data shown are representative of three similar independent experiments that assessed BθOM CD4+ T cell activation across a range of doses of peptides (A) or indicated *B. thetaiotaomicron* strains (B). In (C) the bar shows the median and each point represents an individual biological replicate. Note, the data for "*B. theta*-VPI-5482$^{\Delta tdk\Delta BT4295}$ and *B. theta*-VPI-5482$^{\Delta tdk\Delta BT4295::BT4295}$ in panel (B) are the same data presented in Figure 4B; all stimulations were performed concurrently.

1110

1111

1112

1113

1114

1115

1116

1117

1118

1119

1120

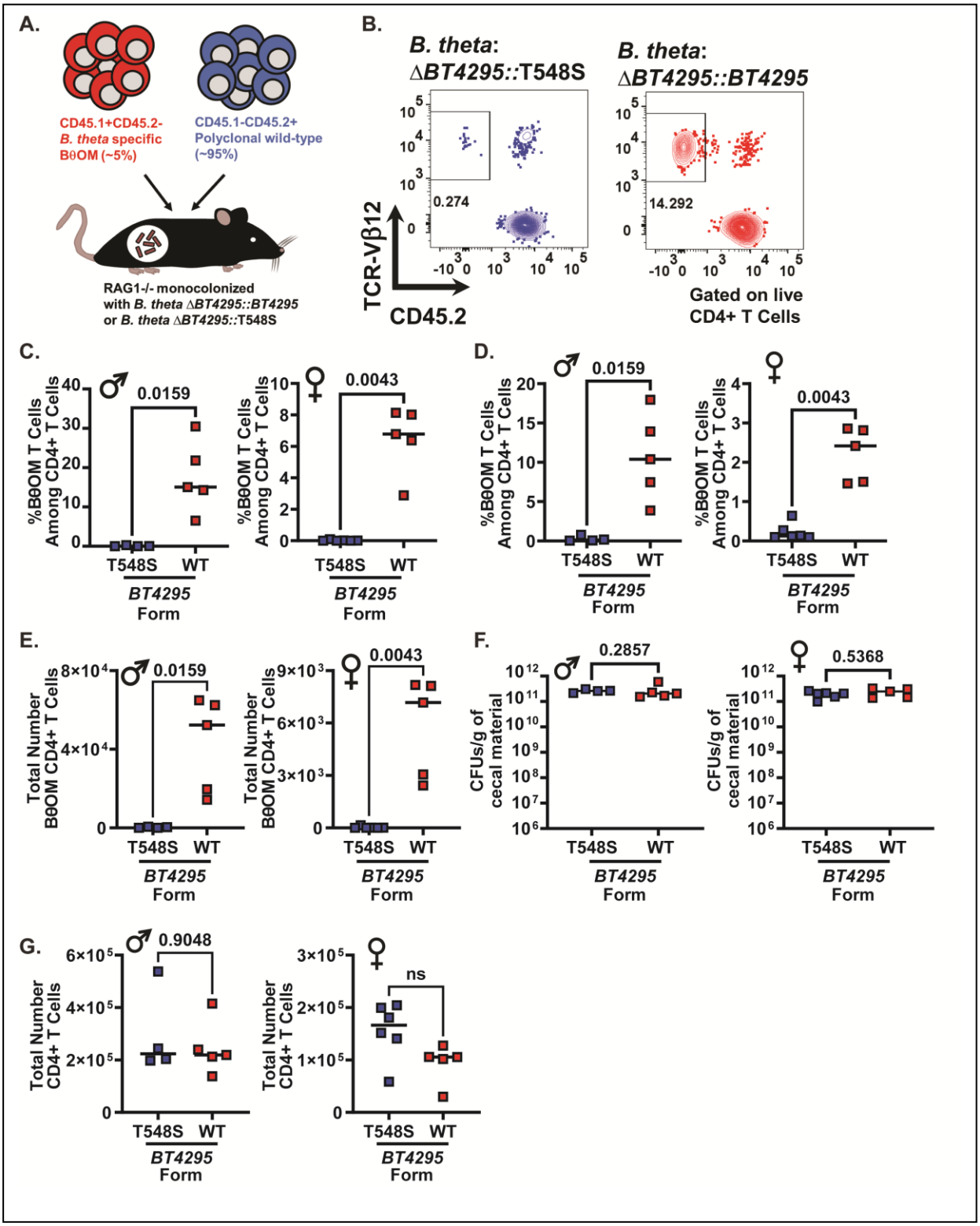

1121

1122

1123

Figure 6-An altered peptide ligand for BθOM CD4$^+$ T cells in *B. theta*-dnLKV9 mediates immune evasion *in vivo*

Naïve BθOM CD4+ T cells were mixed with unfractionated wild-type polyclonal CD4+ T cells and adoptively transferred to gnotobiotic RAG1-/- mice that had been colonized for ~2 weeks with the indicated strain of *B. theta*. ~3 weeks later the accumulation of BθOM CD4+ T cells were quantified

(A) Schematic outlining experimental design for cell transfer.
(B) Representative flow cytometry plots showing BθOM CD4+ T cell accumulation in the colon of the indicated groups of recipient mice (data shown is from male mice).
(C) Graph shows the proportion of BθOM CD4+ T cells among all CD4+ T cells in the colon for both male and female recipients ~3 weeks post cell transfer.
(D) Graph shows the proportion of BθOM CD4+ T cells among all CD4+ T cells in the spleen for both male and female recipients ~3 weeks post cell transfer.
(E) Graph shows the total number of BθOM CD4+ T cells in the colon of male and female recipients ~3 weeks post cell transfer.
(F) Graph shows the colonization levels of *B. theta* as quantified by enumeration of colony forming units (CFU) in the cecum ~5 weeks post colonization, ~3 weeks post cell transfer.
(G) Graph shows the total number of CD4+ T cells, encompassing BθOM and wild-type CD4+ T cells in the colon of both male and female recipient mice ~3 weeks post cell transfer.

Bars show the median and data points represent individual mice. Male and female cohorts represent two independent experiments. Statistical significance was determined via Mann-Whitney test. P values <0.05 were considered to be statistically significant. Symbols indicate the sex of the mice used: ♂ for male and ♀ for female.

1124

1125

1126

1127

1128

1129

1130

1131

1132

1133

1134

1135

1136

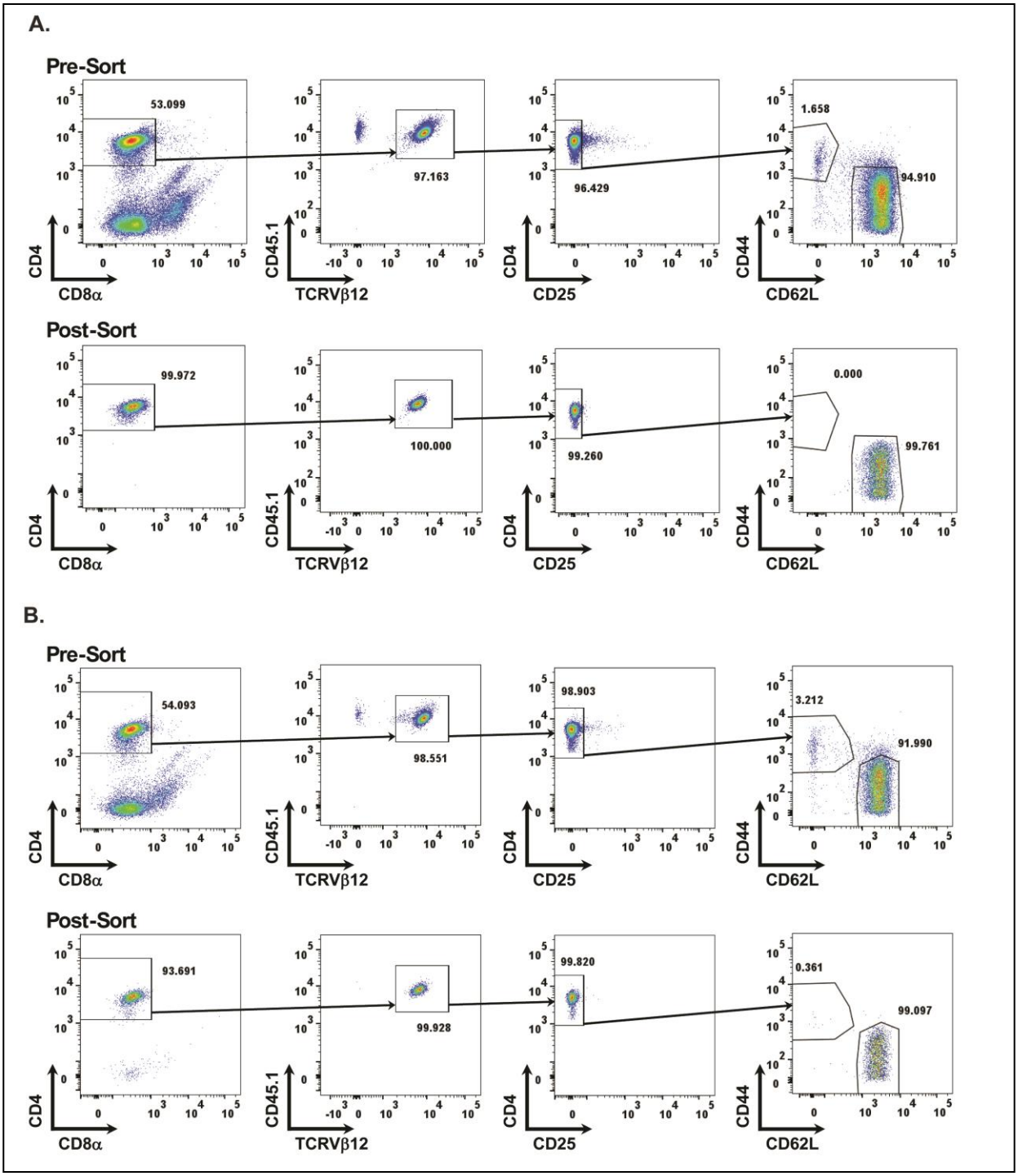

Supplementary Figure 1-Gating strategies for purification of cells by flow cytometric based cell sorting

Naïve BθOM CD4+ T cells for *in vivo* adoptive transfer experiments were purified by flow cytometric based cell sorting. Representative pre- and post- sort frequencies are shown from two independent experiments.

1137

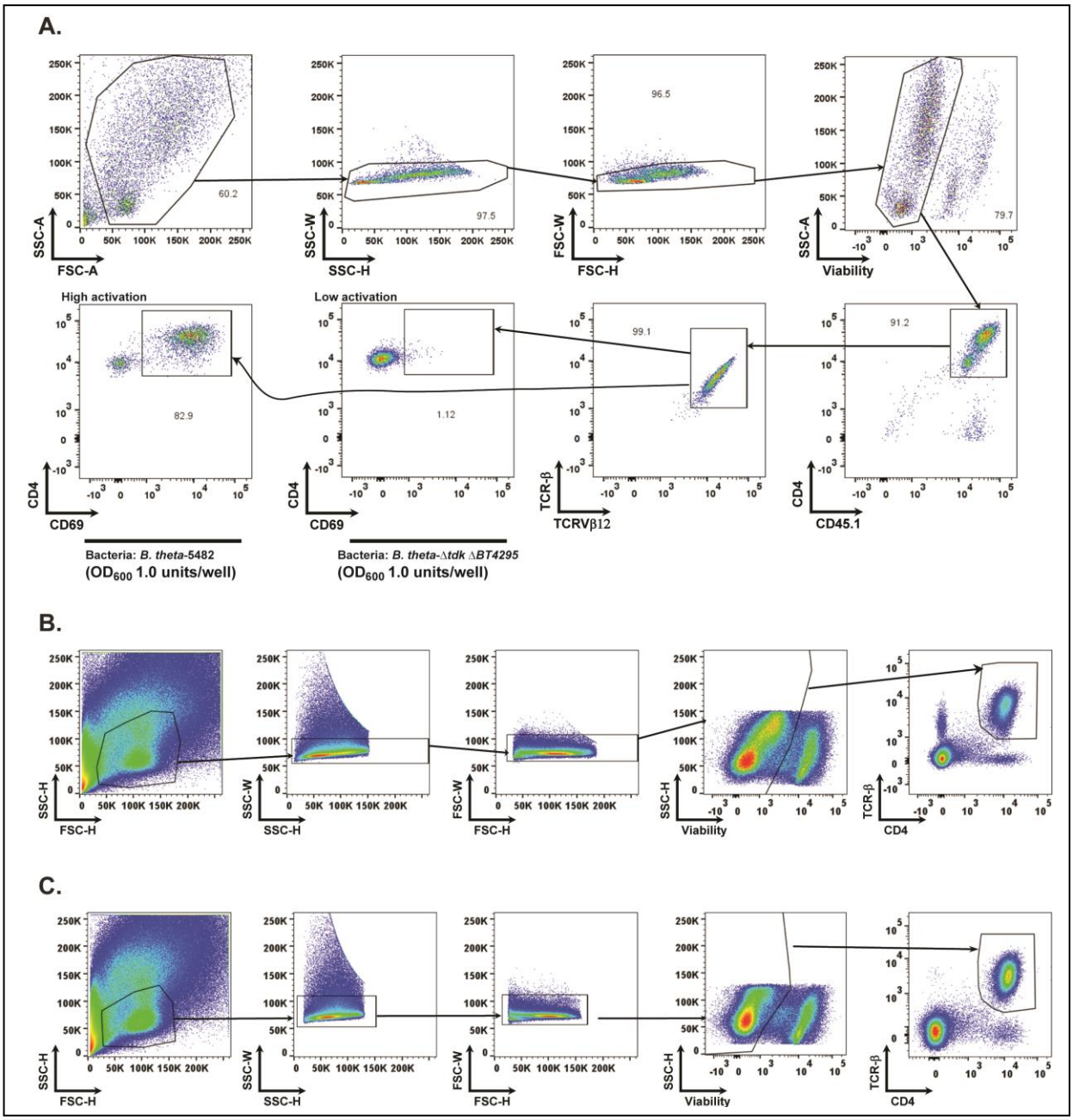

Supplementary Figure 2-Gating strategies for purification and analysis of BθOM CD4+ T cells by flow cytometric based cell sorting and flow cytometry respectively.

BθOM CD4+ T cell activation following *in vitro* stimulation or following *in vivo* adoptive transfer was assessed via flow cytometry. Shown are representative gating strategies used to phenotype BθOM CD4+ T cells from these assays.

(A) Strategy for assessment of *in vitro* stimulation of BθOM CD4+ T cells
(B) Strategy for assessment of BθOM CD4+ T cells in experiments comparing *B. theta*-VPI-5482 and *B. theta*-dnLKV9 *in vivo*.
(C) Strategy for assessment of BθOM CD4+ T cells in experiments comparing *B. theta*$^{\Delta tdk\Delta BT4295::BT4295}$ (WT) *or B. theta*$^{\Delta tdk\Delta BT4295::T548s}$ (T548S) *in vivo*.

1138